CHALMERS

Effect of nanotopography on bacterial adhesion and EPS production

Master of Science Thesis in the Master Degree Program, Biotechnology

NEDA NAJAFINOBAR

Department of Applied Physics

CHALMERS UNIVERSITY OF TECHNOLOGY

Gothenburg, Sweden, 2011

Master of Science Thesis in the Master Degree Program, Biotechnology

Effect of nanotopography on bacterial adhesion and EPS production

Neda Najafinobar

Supervisors:

Mats Hulander

Professor Hans Elwing

Department of Cell and Biology/Interface biophysics, University of Gothenburg, Sweden

Examiner:

Associate Professor Julie Gold

Department of Applied Physics, Chalmers University of Technology

Abstract

Bacterial infection after surgeries is a serious problem that cannot be treated by traditional antibiotics because of antimicrobial resistance and biofilm formation. Recently, a new coating (Bactiguard coating) has been developed that is able to reduce the infection significantly without compromising biocompatibility. This coating is comprised of nanosized deposits of Ag, Pd, and Au. It is not clear how this coating reduces infection. Therefore, this study aims to investigate how bacterial adhesion and production of extra cellular substances (EPS) are affected by surface nanotopography. However, the exact mechanism of action is not yet fully understood. The studied topographies are a flat and nanostructured gold surfaces. The fabrication method used was self-assembly with 20 to 30 nm gold nanoparticles. For the cell study *staphylococcus epidermidis*, was used. Bacterial cell adhesion and the formation of EPS were investigated. FilmTracer TM SYPRO Ruby biofilm matrix stain was used in order to stain EPS.

In order to characterize the surfaces contact angle and scanning electron microscopy (SEM) were used. Dynamic light scattering and spectrophotometry was applied to analyze the size of the particles. SEM analyzed the number of cells attached on both surfaces. No difference was observed on the number of cells attached on both surfaces. Quartz Crystal Microbalance with Dissipation Monitoring (QCM-D) was used to study the adhesion of bacteria and the production of EPS in real time. The results show that dissipation is lower on nanostructured surface that can be due to firmly attachment of bacterial cells on the surface and more production of EPS. Therefore, bacteria seem to behave differently when adsorbing on a flat or nanostructured surface.

List of abbreviation

SEM- Scanning Electron Microscopy

AFM – Atomic force microscopy

QCM-D- Quartz Crystal Microbalance with Dissipation Monitoring

PBS – Phosphate buffer saline

LB- Lysogeny broth

DLS- Dynamic Light Scattering

EPS- Extracellular polymeric substances

S-layer- Surface layers

PEG- Polyethylene glycol

S. epidermidis- Staphylococcus epidermidis

S. aureus- Staphylococcus aureus

S. salivarius- Streptococcus salivarius

P. aeruginosa- Pseudomonas aeruginosa

RSA - Radom sequential adsorption

SPM- Scanning probe microscopy

Contents

1. Introduction 7
2. Aims and approach of the project 8
3. Background 8
3.1. Infection 8
3.2. Bacteria 8
3.3. Surface components of bacterial cell 9
3.4. Bacterial adhesion 10
3.4.1. Physicochemical interactions between bacteria and the surface (Phase one) 10
3.4.2. Molecular and cellular interactions between bacteria and surfaces (Phase two) 11
3.5. Factors affecting bacterial adhesion 11
3.5.1. Environment 11
3.5.2. Bacterial cell membrane 11
3.5.3. Hydrophobicity 11
3.5.4. Protein adsorption 11
3.5.5. Chemistry of the surface 12
3.5.6. Nanotopography 12
3.6. Gold nanoparticles 14
3.7. Synthesis of gold nanoparticles 14
3.7.1. Turkevich method 14
3.7.2. Brust method 15
3.7.3. Martin Method 15
3.8. Self-assembly methods to grow nanocolloidal gold film 15
3.9. Effect of ionic strength of particle solution on particle coverage on the surface 17
3.9. Biomarkers 18
3.9.1. FilmTracer ™ SYPRO Ruby biofilm matrix stain 18
3.10. Material analysis 18
3.10.1. Scanning electron microscopy (SEM) 18
3.10.2. Dynamic light scattering (DLS) 19
3.10.3. Spectrophotometer 19
3.10.4. Contact angle 20

3.11. Cell analyzing methods 21
3.11.1. Fluorescence microscopy 21
3.11.2. Quartz Crystal Microbalance with Dissipation Monitoring (QCM-D) 21
4. Materials and methods 23
4.1. Preparation of gold nanoparticles 23
4.2. Preparation of nanostructured surfaces 23
4.3. Surface characterization 24
4.4. Bacterial strain and culture condition 25
4.5. Determination of bacteria concentration 25
4.7. Scanning electron microscopy 25
4.8. Fluorescence microscopy 25
4.9. QCM-D experiments 26
5. Results 26
5.1. Characterization of the surface 26
5.1.1. Dynamic light scattering 26
5.1.2. Spectrophotometry 27
5.1.3. Scanning electron microscopy 27
5.1.4. Contact angle 28
5.2. Cell observation 29
5.2.1. Scanning electron microscopy 29
5.2.2. Fluorescence microscopy 32
5.2.3. Quartz Crystal Microbalance with Dissipation Monitoring (QCM-D) 33
6. Discussion 36
6.1. Nanostructured gold surfaces 36
6.2. Scanning electron microscopy (SEM) 37
6.3. Fluorescence microscopy 38
7. Conclusion 40
8. Suggestions for further experiments 40
9. Acknowledgements 42
10. References 43
11. Appendix: 48

1. Introduction

Today millions of people use biomaterials to support or restore their function. Although biomaterials have contributed to great improvement in medicine, biomaterial-associated infections are dramatic threat to human body. For instance, todays close to 500,000 hip and knee replacements are operated worldwide every year, while 5% to 10% of total knee surgeries annually end with failure and in most cases the reason is biomaterial-associated infections [1]. The consequences of these infections are quite high for the patient because most of the time there is no choice but removing the implant. The estimated cost in order to treat these infections is almost $62,100 while for non-infected patient this cost reduces to $8600 [2]. Hence, reduction of biomaterial-associated infections is of great importance after implantation [2].

One way to prevent infection is the usage of antibiotic around the implant immediately after the surgery. In order to achieve this goal, biomaterial has been design that can release antibiotic after implantation. As the concentration of antibiotic should be high in order to be effective, this method can cause systemic toxicity and has several side effects [3]. Moreover, the more time pass from the surgery, the less the antibiotic is effective because of development of antimicrobial resistance among bacteria [4]. There are also other investigations to reduce the infection. For instance, it has been shown that titanium surfaces modified with hydroxyapatite (HA) sol-gel containing silver increase the antibacterial activities and reduce bacterial adhesion on the surface [5].

Moreover, according to several studies, surface properties including micro and nano-topography can affect bacterial adhesion and production of extracellular polymeric substances (EPS) [6, 7]. Extracellular polymeric substances are a matrix of polymers and the main components of EPS are polysaccharides, glycoproteins, proteins, phospholipids and nucleic acids [8]. This matrix not only helps biofilm to adhere to the surface but also protects bacteria against phagocytosis and causes chronic infection [9]. Surface composition can be modified through appropriate micro/nano fabrication techniques to study the influence of the properties on bacterial adhesion and production of EPS [10].

Bactiguard coating is a new achievement that is able to reduce the infection significantly without compromising biocompatibility. This coating is comprised of nanosized deposits of Ag, Pd, and Au and is in clinical use on urinary catheters. It is not clear how this coating reduce infection and therefore, the aim of this study is to investigate if nanotopography can contribute in reducing the infection and be the possible mechanism behind the observed responses of the bactiguard coating [11].

There are many ways one could measure how bacteria respond to a specific surface. A commonly used model system to study bacterial adhesion is *Staphylococcus epidermidis* [12-15]. A way to investigate the adhesion of bacteria is to measure the number of cells attaches on the surface and the amount of EPS are produced by the means of specific biomarkers and fluorescence microscopy. Moreover, Scanning electron microscopy (SEM) can provide good information about the morphology of the cell. In addition to, a relatively new analytical method named Quartz Crystal Microbalance with Dissipation Monitoring (QCM-D), which has been

used in this study, provides information about the changes of the mass absorbed on the surface and its viscoelasticity in real time.

The ultimate goal is to learn how and why nanotopography influences bacterial adhesion. By understanding the underlying cellular mechanisms, fabrication methods of nanostructured surfaces become more sophisticated and medical implants with desired host response can be fabricated.

2. Aims and approach of the project

The aim of this study was to study how a gold surface with nanometer sized topography influences bacterial adhesion and EPS production. The bacterium of use was *Staphylococcus epidermidis* and the goal was to observe the difference on bacterial adhesion between flat and gold nanostructure surface. The three main areas of interest are:

- Fabrication of nanostructured model surfaces
- Cell culture of *staphylococcus epidermidis*
- Adhesion of bacteria and EPS production

3. Background

3.1. Infection

The exact definition of infection is the growth of a parasitic organism in the body. An infected person has a pathogen called parasitic organism in his body which getting its nourishment from him and reproduce inside the body. Viruses, bacteria and fungal can cause infection. Although most of the bacteria are harmless or even beneficial for human body, one percent of bacteria can cause chronic infections [16].

Infections become a main barrier when it comes to long-term use of implanted or intravascular devises such as vascular catheters and joint prostheses. Infections are mostly caused by the bacteria *Coagulase Negative Staphylococci* (CoNS), *S. epidermidis*, *S. aureus*, *Pseudomonas aeruginosa*, *E.coli*, *Streptococci* and *Candida sp* [17].

3.2. Bacteria

The bacterium is a prokaryotic cell with micrometer length that exists mostly together in millions. The shape of bacteria can be divided in three main categories, spherical called cocci, rod shaped which are known as bacilli and spiral named spirilla [18].

A group of bacteria that cause infection in different tissues within the body is *Staphylococcus*. As this group of bacteria looks like a bunch of grapes or small round berries under the microscope, it has been named staphylococcus which comes from Greek staphyle, meaning a bunch of grapes, and kokkos, meaning berry. There are more than 30 various kinds of *Staphylococci* which can cause infection in human body and the most important one is named *Staphylococcus epidermidis* [19]. This species is small (~ 1 μm in diameter) and gram-positive staphylococcal that has a high tendency to form cluster. Unlike *S. aureus*, *Staphylococcus epidermidis* grows rapidly on blood agar and is not destructive on blood agar plates. On another word*, S. epidermidis* is not able to congeal blood because it does not produce an enzyme named coagulase; hence its name is coagulase-negative staphylococci. It has been observed that this species is the main contributor

in the infection of intravascular catheters, cerebrospinal fluid shunts, prosthetic valves, orthopaedic devices, artificial pacemakers, chronic ambulatory peritoneal dialysis catheters, and vascular grafts [19].

3.3. Surface components of bacterial cell

Surface components have a fundamental role to able bacterial cells to communicate with their environment. Cells need their surface components in order to assess the environment and respond in an appropriate way to be able to survive. Moreover, the molecular composition of the cell membrane including Fimbriae (Pili), S-layers, Capsule, Slime Layers and Flagella can determine the surface properties of bacteria [20].

Fimbriae: are appendages that exist on the membrane of bacterial cell. They are 1 to 20 microns in length, thin and hairlike and because they are protein (pilin) they have antigenic properties. While a few cells use fimbriae for motility, the main function of fimbriae is to facilitate the attachment of bacterium to other cells and to the surface. The other appendages present on the surface of bacteria are named pili which are quite similar to fimbriae in structure but smaller. They are also used in the process of bacterial adhesion to the surface [20].

Flagella: are composed of thready protein structure with 20 nanometers in diameter. The function of flagella is to facilitate the motility of bacterial cells. The rotation of flagella by motor apparatus placed in plasma membrane helps the cell to move through the fluid environment. Propulsion of the flagella is driven by the proton motive force or chemiosmotic potential of the bacterial membrane. During chemotaxis a bacterium can move towards or away from certain chemicals if they are useful nutrients or harmful substance respectively. A clear example is aerotaxis when bacteria swim toward or away from O_2 based on their need [20].

Surface layers (s-layer): exist on the surface of many bacteria that completely cover the cell by the formation of porous lattices with protein subunits. S-layers have fundamental biological functions including antigenic properties, cell adhesion and protection from feeding by protozoa or phagocytes [21].

Capsule: is a polysaccharide layer that exists on the outer membrane of most bacteria. As this layer prevents phagocytosis because of its slipperiness and fragility properties, it increases the potential of bacteria to cause diseases and is considered as virulence factor. This layer not only reduces phagocytosis but also because it contains water, that protects bacteria against desiccation [20].

Slime layer: is an extracellular substance produced by bacteria and likely leaves the cell membrane after dissemination in fluid environment [22]. Extracellular slime is believed to play a main role as an ion exchange resin for extra nutrition, in order to prevent phagocytosis and to interfere the response to antibodies; hence it is an important factor in the development and persistence of biomaterial infections [23].

Extracellular polymeric substances (EPS): are a matrix of polymers and the main components of EPS are polysaccharides, glycoproteins, proteins, phospholipids and nucleic acids [8]. It has been reported that EPS highly contribute in aggregation and adhesion of cells, formation of biofilm and protection of cells from antimicrobial agents. This matrix not only helps biofilm to adhere to the surface but also protects bacteria against phagocytosis and causes chronic infection [9].

Biofilm: is a complex three-dimensional structure that includes bacteria and extracellular materials and it is produced at the last stage of bacterial adhesion [22]. In the medical field, formation of biofilm on a solid surface is remarkably dangerous as biofilm has high resistance to be killed by antimicrobial agents. There are many advantages provided by biofilm for bacteria such as providing nutrition for bacteria or protecting the bacteria from antimicrobial agents or host defense [24].

3.4. Bacterial adhesion

It is suggested that once a surface is implanted in human body, a competition starts between tissue cells and bacteria to attach to the surface. In this competition either tissue cells occupy the surface and prevent bacterial colonization or bacteria adhere to the surface and form biofilm. Bacterial adhesion not only is influenced by specific receptors and outer membrane molecules on the bacterial cell surface, but also by the atomic geometry and electronic state of the biomaterial surface [23].

According to the observations on adhesion of bacteria in marine environment, it is assumed that bacterial adhesion is two phase processes including initial, reversible attachment without metabolic energy (phase one) followed by a time dependent and irreversible adhesion involving metabolic energy that place the adherent bacteria in a three-dimensional matrix (phase two) [25].

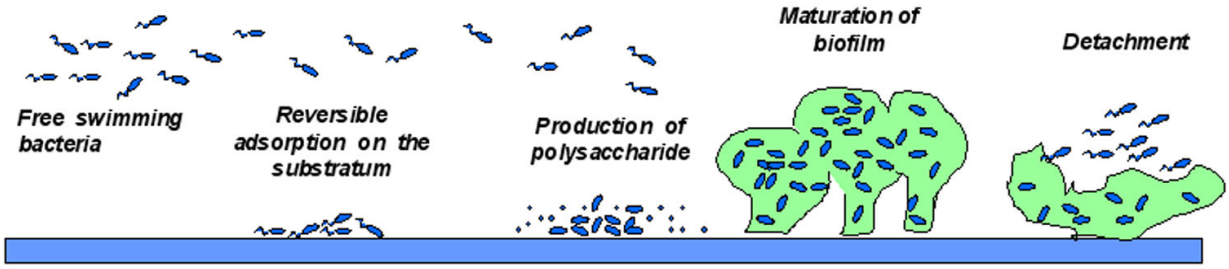

Figure 1. This image illustrates the dynamic process of bacterial adhesion and biofilm formation [26].

3.4.1. Physicochemical interactions between bacteria and the surface (Phase one)

The initial step of bacterial adhesion can be described by DLVO theory as bacteria are in the range of colloidal particles in size (0.5-2nm). DLVO theory describes the interaction of colloidal particles with a surface based on the summation of their Coulomb and van der Waals interactions [25]. Coulomb force is considerably dominant when bacteria are far from the surface while van der Waals interaction increases sharply near the surface. The physical interactions are explained as long and short-range interactions. The long-range interactions including Brownian motion, gravitational forces or hydrodynamic forces (>50 nm) are nonspecific and transport the bacteria close to the surface while short-range interactions including chemical bonds, ionic and dipole interactions (<5 nm) become effective when bacteria are close to the surface [17]. When the bacterial cells come near the surface, because bacterial cells and natural surfaces are usually negatively charged in aqueous solution, there is a repulsive electrostatic energy due to overlapping of the electrical double layers of bacterial cells and the surface [25]. Therefore, the bacteria need to surmount energy barrier exists on the surface in order to attach on the surface. In this step, bacteria either produce extracellular polymeric substances (EPS) or use nanofibers such as pili and flagella in order to make a bridge to the surface and adhere irreversibly [25].

3.4.2. Molecular and cellular interactions between bacteria and surfaces (Phase two)

In phase two, bacteria attach permanently to the surface through molecular-specific reactions between bacterial surface structures and substratum surfaces [17]. Once bacteria attach irreversibly, they start to divide and produce EPS. In the next step, biofilm is formed by the reproduction of bacteria and accumulation of EPS. EPS matrix is capable of trapping nutrients for bacteria from water, as it carries both charged and neutral polysaccharide groups [27]. After formation of biofilm, bacteria can communicate with each other through their membrane organelles and biochemical signals. In most cases after formation of biofilm second surgery is required in order to remove the implant [6].

3.5. Factors affecting bacterial adhesion

In order to control the process of bacterial adhesion, knowledge about the certain bacteria, environmental conditions including the presence of serum proteins and the surface characteristics is essential. Better understanding of how these factors affect bacterial adhesion would make it possible to control the adhesion process [22].

3.5.1. Environment

Generally, some environmental factors including bacterial concentration, time period of exposure, temperature and presence of antibiotics affect adhesion of bacteria to the surface [17]. For instance, it has been shown that the longer the exposure time is the more bacteria adhere to the substrate surface until they reach a saturation level which varies for each type of surface and each type of bacteria [22].

3.5.2. Bacterial cell membrane

Surface components of bacterial cell are remarkably dependent on bacterial species and can highly affect the bacterial adhesion process and biofilm formation. The presence of appendages such as flagella or pili, the amount of extracellular polymeric substances produced by the bacteria and the specific membrane receptors are the factors that can highly influence the adhesion of bacteria. For instance, the types of bacteria that have flagella on their membrane are more motile compare to those that do not have flagella. Moreover, bacteria with fimbriae, pili or curli on their membrane can attach to the surface easier as they can use these components to make a bridge to the surface [6].

3.5.3. Hydrophobicity

Non- specific macroscopic surface properties including surface free energy, surface charge and hydrophobicity mediate the adhesion process in short separation distances (>5nm) [17]. Hydrophobicity can affect the adhesion process by removing the vicinal water film between the cell surface and the substratum. On another word, hydrophobic groups use their dehydrating capacity to remove the water and aid surface appendages to attach to the surface [28]. In low-ionic-strength environments, the microbial surface hydrophobicity and charges are of greater importance [29].

3.5.4. Protein adsorption

The adhesion of bacteria can increase or reduce in the presence of certain protein in the medium. For example, in the study done by E. Vaudaux, Plasma protein adsorption on polymeric biomaterials was investigated in order to define the role of host protein on the adhesion of

S.aureus. It has been shown that fibrinogen or fibrin as a very active plasma component increases *S.aureus* attachment in a short-term blood-material interaction [30].

In order to influence bacterial adhesion, dissolved protein should affect either the bacterial surface or the surface of the implant. For instance, attachment of a protein with appropriate isoelectric point on the surface of an implant might be able to neutralize surface charge density and increase the numbers of bacteria that attach on the surface. On the other hand protein attachment on the surface can reduce bacterial adhesion through non-electrostatic repulsion mechanisms, such as steric exclusion. Moreover, the more dissolved proteins exist in the medium the higher the viscosity will be. High viscosity might affect the movement of the bacteria and consequently might affect the bacterial adhesion [31].

3.5.5. Chemistry of the surface

It has been shown that chemistry of the surface can influence bacterial adhesion to some extent. For instance, it has been observed that PEG (Polyethylene glycol)-coated surfaces can reduce bacterial adhesion as compared to their control samples over a short period of time such as *S. epidermidis*, *S. aureus*, *S. salivarius*, *E. coli*, and *P. aeruginosa* on PEG-brush coated glass [27].

Moreover, chemistry of the surface can influence the bacterial adhesion through affecting protein absorption. For instance, it has been observed that PEG suppress the adhesion of *S. epidermidis* for 24 h in PBS, for 48 h in urine, and for only 4 h in saliva because of various proteins attached on the surface from the medium. PEG-coated materials are able to suppress the adsorption of nonspecific protein and short-term bacterial adhesion, while they do not affect long-term biofilm formation significantly [27].

3.5.6. Nanotopography

To design a surface that hinder the adhesion of bacteria, understanding the behavior of bacteria on nanostructured surfaces is essential. It has been observed that cells not only chose their direction but also modify the production of EPS in response to nanotopography [7]. For instance, it has been shown that the bacterial adhesion increases and EPS production decreases when parameters that characterize topography are in the same order with bacteria dimension [6]. Moreover, some interesting results have demonstrated that nanostructured materials can promote human osteoblasts function while can hinder *S.epidermidis* colonization [32].

The exact mechanism of how bacteria response to micro and nanotopography is not yet well understood. Many factors influence the response of bacterial cells to surface topography including the height, width, shape and organization of the nanofeatures [6]. For instance, one investigation has studied the primary colonization of three bacteria on titanium surfaces with different micro-topography. The results have demonstrated that with the increase in surface roughness, the adhesion of bacteria increases as well [6, 33]. Moreover, the adhesion of *Pseudomonas fluorescens* was studied on gold nanostructure surfaces by Diaz et al [6, 34]. Three different types of nanostructured surfaces were prepared, smooth, structured surfaces with random nanometer size topography and structured with grooves 750 nm wide and 120 nm deep. The results indicate that initial stage of bacterial adhesion is affected considerably by ordered surfaces and the formation of ordered aggregation is prevented. Moreover, it has been observed that structure of the surface can influence the size and shape of bacteria, their interaction with each other, and also the orientation of cellular substructures involved in motion [6, 34].

Based on a study done by Mitik-Dineva et al. on the impact of nanotopography on adhesion of bacteria, it has been shown that nanotopography can affect different parameters of bacterial adhesion[6]. The surfaces in the study done by Dineva were non- etched and etched glass surfaces obtained by chemical etching, Ra (and Rq), Rmax and Rz after etching were (1, 8 and 10 nm, respectively). Although it is expected that increase in roughness results in increase of bacterial adhesion, this study demonstrates that a decrease in size of nanotopographical feature leads to an increase in the number of attached bacteria [6]. The most important finding of all these studies is that bacteria may be far more susceptible to nanoscale surface roughness than was previously thought [35].

The interaction between cell membrane structures and nanostructured surfaces is an important issue that needs further investigations. There are a few published studies on this subject because of two reasons. First, the description of bacterial structures is quite new and not fully discovered. Secondly their small size makes them hard to investigate. Although the precise mechanisms of how nanotopography affects bacterial adhesion are quite unknown, there are some explanations based on the results that have been obtained so far. It is proposed that because of the higher surface area available on nanostructured surface, protection from shear forces and chemical changes that cause preferential physicochemical interactions; bacteria preferentially stick to rougher surfaces. This may be able to explain why the number of attached bacteria is higher on structured surface compare to flat ones. On the other hand, topography does not always increases adhesion of bacteria on the surface due to an energetic barrier exist on the surface and also changes in morphology of bacterial cell which is needed in order to attach to the surface [6, 36].

Moreover, on the nanoscale it is possible for the bacteria to improve binding energy with topographical features through its cell wall features such as pili, fimbriae or other proteins or carbohydrate molecules found on the cell wall because of their small size. For instance, it has been shown that bacteria with flagella on their membrane colonize micro structured surfaces more compared to the bacteria without flagella. This can be because of the ability of flagella to help bacteria to sense topographical feature and move into the grooves or crevices [6]. Based on the fact that bacteria with different membrane structures have different ability to move, sense and anchorage to a surface, it become clear that bacterial species has large impact on the response of bacteria to nanotopography [6, 36].

Although the small size of the bacteria compare to eukaryotic cells is a suitable factor for bacteria to interact with topographical features, the fact that bacteria are less deformable than eukaryotic cells and keep their shape after attachment on the surface might hinder the interaction of bacteria with the nanostructured surfaces [6].

It is needed to consider that nanotopography might change surface energy and surface chemistry. One very clear example is the changes in hydrophobicity on nanostructured surface compare to the bulk that has been explained by two different theories. Based on the theory introduced by Wenzel, both hydrophobicity and hydrophilicity are increased due to the nanotopography. The surface that is hydrophobic becomes more hydrophobic and the surface which is hydrophilic becomes more hydrophilic [37]. Based on the other theory developed by Cassie and Baxter, the nanostructured surface is more hydrophobic compare to the bulk due to lotus effect. This increase in hydrophobicity is due to the higher air content of the nanostructured surface and consequently higher surface contact angle [37]. Careful attention much be paid to these

differences since any small differences in surface chemistry can have impact on adhesion of bacteria and influence the effect of nanotopography [6, 38].

3.6. Gold nanoparticles

Today because of the wide application of nano metal particles especially gold nanoparticles in the areas of chemistry, biotechnology, electronics and medicine, these particles have attracted the attention of scientists. Gold nanoparticles (AuNPs) are of great interest because of their unique properties including excellent biological compatibility, controllable morphology and size dispersion, high stability, and unique optical, catalytic and electronic properties. These properties make gold nanoparticles an attractive material for biosensors, chemisensors and electrocatalyst [39].

3.7. Synthesis of gold nanoparticles

There are many different types of gold nanoparticles that are different in size, shape and physical properties (fig. 2). The type studied widely is gold nanospheres and subsequently, nanorods, nanoshells and nanocages are the other types of gold nanoparticles. Moreover, SERS nanoparticles are the other type of gold nanoparticles with good surface enhanced Raman scattering properties [40]. Producing gold nanoparticle with suitable size distribution, appropriate stability and high activity is very important. There are many types of synthesis with different end product. Some of them are mentioned below [41].

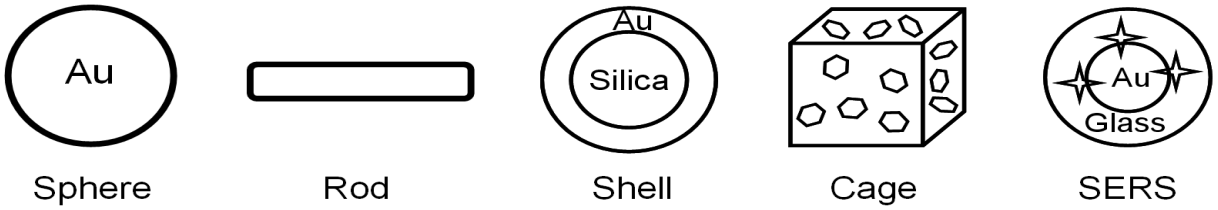

Figure 2. Different types of gold nanoparticles [40].

3.7.1. Turkevich method

The most commonly method used to make gold nanoparticles has proposed by Turkevich at 1951 and refined by Frens at 1973. This method also has been used in this research. This method is a single-phase water based method that uses citrate as reducing agent in order to reduce gold or silver salt in the solution. After formation of nanoparticles, citrate ions gather around particles and negatively charge the particles; Hence due to electrostatic repulsion between particles, particles do not aggregate. This method is capable of producing monodisperse and nanospheres in a wide range of sizes from 9 to 120 nm with reasonable size distribution. The particles size can be influenced by several factors such as citrate/gold ratio, PH, and temperature. It was observed that small amount of citrate lead to large particle and low temperature lead to final nanoparticles with larger diameters and irregular shape[41].

As gold ions are reduced in the solvent at 60-80 ^{o}C, the color of the medium changes from bluish-purple in the early stages to deep red at the end stage of the reaction [42]. These changes in the color of the solvent indicate that at the early stage, there are aggregations of small particles in the medium while with time the small particles detach from each other and grow to average diameter of 10 to 50 nm [43, 44].

3.7.2. Brust method

This method was first introduced by Brust at 1990 which uses thiols in order to synthesize gold nanoparticles. This method inspired by the two-phase system used by Faraday in 1857 and has been improved through the use of a phase transfer reagent such as tetraoctylammonium bromide [42, 45]. Reactions involve in Brust synthesis are categorized as three reactions: phase transfer of a gold salt, reduction of Au (III) to Au (I) and Reduction of Au (I) to Au (0). In this method a monolayer of thiolates is used in order to stabilize gold nanoparticles. These particles have many advantages that the most important one is that these nanoparticles can be stored for long time or re-dissolve in solvent because of their extraordinary stability. Moreover, they can undergo more synthetic manipulation such as surface functionalization. Although these robust nanoparticles have attracted the attention of many researchers, the size distribution of these particles (normally between 2 to 5 nm) is a major disadvantage. It has been observed that large amount of thiol/gold ratios and fast addition of the reductant in cooled solution lead to more monodispersed and small nanoparticles [45].

3.7.3. Martin Method

This recently discovered method use NaBH4 to reduce HAuCl4 in water in order to produce naked gold nanoparticles. In the following step, naked gold nanoparticles are covered by a monolayer of 1-dodecanethiol and then with shaking a mixture of water, acetone and hexane, these nanoparticles are transferred to hexane phase and all the byproducts are remained in water acetone phase. Therefore, no post-synthesis cleaning is required for particles. This method is very important for practical application because of its advantages such as being simple, cheap, greener and easy to adopt. Moreover, unlike Brust method there is no difficulties to remove the phase-transfer agent. In this method the size distribution is almost monodisperse and the diameter of the nanoparticles can be adjusted very precisely from 3.2 to 5.2 nm [46].

3.8. Self-assembly methods to grow nanocolloidal gold film

Nowadays, the attention has attracted different fabrication methods. It has been observed that fabrication methods like electron beam lithography, which is a top down method, are being replaced by bottom up methods including self-assembly of nanocolloidal particles into larger arrangements. Much of the efforts these days are being devoted on assembling gold nanocolloidal particles into either disordered or highly ordered structures [47].

There are many different methods to assemble gold nanoparticles into structures. The most commonly applied method that has been applied in this project is attachment of gold nanoparticles to chemically modified surfaces. The biggest advantage about this method is that it can be applied for different substrate (glass, metal, Al2O3), geometry (planar, cylindrical), functional group (-SH, -P (C6H5)2, -NH2, -CN), and particle diameter (2.5-120 nm) [48]. Surfaces that are functionalized with amino or thiol group can be generated by attachment of either biofunctional amino-thiol or dithiol molecules onto gold substrate with immersion of the substrate in a solution of the functionalizing substance or evaporation/sublimation of the amino or thiol compounds. It is better to use molecules with short chain, as long chain molecules with high degree of freedom can attach to the surface from both ends. On chemically modified gold nanoparticles attach very firmly and there is no desorption after the attachment. Moreover, by applying this method the maximum surface coverage corresponding to an random sequential adsorption (RSA) event is approximately 55% [47]. In this project the surfaces were chemically modified by the attachment of cysteamine (a thiol-amino molecule). The cyteamine attaches on

the gold surface from its thiol group and then negatively charged gold nanoparticles attach to the positive amino group by electrostatic attraction (fig 3).

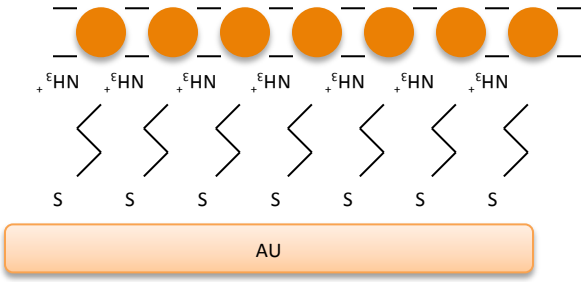

Figure 3. In this image cyteamine attaches to the gold surface from its thiol group while it's positively charged amino group attaches to negatively charged gold nanoparticles.

There is another method that is quite similar to the previous described method. In this method thiol molecules with DNA at the end are applied to attach gold nanoparticles to the surface. The main advantage of this method is that by applying different ration of various DNA types, the location and also the density of nanoparticles can be determined [47, 49].

By applying the methods described above only surfaces with one layer of gold nanoparticles can be produced. In order to make multilayer of particles on the surface layer-by-layer (LBL) technique can be utilized (fig 4). After the attachment of first layer of nanoparticles on the surface by applying above methods, a layer of biofunctional molecules including amino-thiol or dithiol are introduced on the surface. These molecules will attach to first layer with their one end and the other end generates new functionalized adsorption sites for new layer of particles [47].

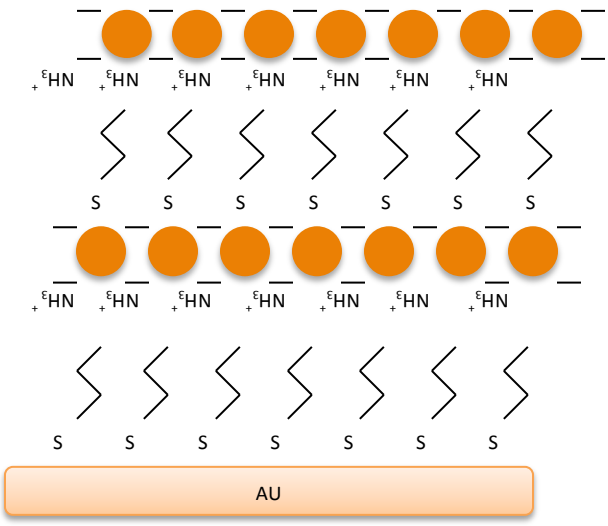

Figure 4. Illustration of layer-by-layer (LBL) technique.

Microcontact printing and scanning probe microscopy (SPM) are other methods that can also be applied in order to locally functionalize substrates. In the former method, polydimethylsiloxane (PDMS) stamp is utilized to cover the predefined areas on the surface with amino-thiol molecules or polyelectrolytes. By this method nanoparticles only adsorb onto the patterned regions covered with amino-thiol molecules. In the scanning probe microscopy (SPM) method, the surface is first covered with molecules with amino end groups and then desired pattern is made by defunctionalizing the surface with an oxidizing agent or by removing the molecules. This method is very slow but by applying this method complicated patterns can be produced [47].

There is another method named electrophoretic deposition that is used to produce a dense monolayer of gold nanoparticles. In this method, an external electric force is utilized in order to bring the particles close to each other. For micrometer sized particles this method has very good results while for nanoparticles more investigation is required [47].

3.9. Effect of ionic strength of particle solution on particle coverage on the surface

Different ionic strength (*I*) of the solution can lead to different particle density on the surface. It has been shown that increase in the ionic strength of the solution results in a dense layer of particles on the surface [50]. The Debye length k^{-1} is the distance which significant charge separation can occur and is the parameter that characterizes the dimension of electric double layer around the particles (fig. 5) [50]. Debye length can be used in order to estimate the hydrodynamic radius r_h of the charged particle in the ion solution. The Debye length κ^{-1} in solution can be calculated according to the Debye–Huckel equation [50]:

$$k^{-1} = \sqrt{\frac{\varepsilon_r \varepsilon_0 k_B T}{2 N_A e^2 I}} \qquad (1)$$

Where I = ionic strength of the solution, e = elementary charge, N_A = Avogadro constant, ε_r = dielectric constant, ε_0 = vacuum permittivity, k_B = Boltzmann constant, T = absolute temperature in kelvins.

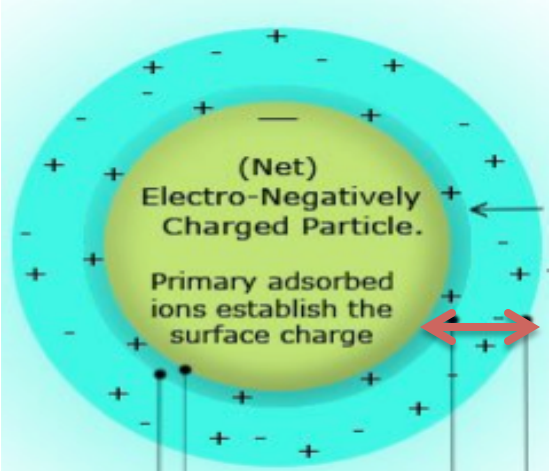

Figure 5. Illustration of electric double layer. The red double arrow represents the electric double layer of this particle [79] .

According to this equation decrease in ionic strength results in increase in Debye length κ^{-1} and leads to larger electric double layer around the nanoparticles. Therefore, a reduced ionic strength results in a larger hydrodynamic particle diameter. In this way the particles occupy more space and the particle coverage on the surface decreases. So it is unlikely that particles touch each other and the risk of having aggregation will be reduced[50].

3.9. Biomarkers

3.9.1. FilmTracer ™ SYPRO Ruby biofilm matrix stain

Lots of efforts have been done in order to present a suitable biomarker to stain biofilm. Presenting a good biomarker for biofilm is difficult because of two reasons. First, biofilm do not spread on the surface homogeneously and consequently stain penetration is not the same on the entire surface. The second reason is that biofilm compose of several components with different chemical and biological properties that are still unknown. The fluorescent stain used in this project was FilmTracer TM SYPRO Ruby biofilm matrix stain. This stain is able to mark most of the proteins in the biofilm such as fibrillar protein, lipoproteins, phosphoproteins, and glycoproteins [51, 52].

3.10. Material analysis

Before using the fabricated material samples in an *in vitro* study with cells, the result of the structure is of great importance to investigate. In order to characterize the surface and determine the size of the nanoparticles, scanning electron microscopy (SEM), dynamic light scattering and spectrophotometry were applied. Nanotopography might influence the hydrophobicity of the surface, which can be investigated by measuring the contact angle.

3.10.1. Scanning electron microscopy (SEM)

A scanning electron microscope (SEM) is a microscope that detects electrons that are scattered or emitted from a specimen surface due to irradiations of the surface with an electron beam. With this technique, it is possible to get images of the three-dimensional structure of the surface of a sample, i.e. to get information about topography, composition and other properties of the surface.

A metal filament produces the electron beam. In the SEM set up the filament is considered function as cathode. The positively charged anode plates attract the electrons from the filament and accelerating them towards the sample. When the electrons pass the anode plates they are condensed by the condenser lens before reaching the objective lens where the beam is focused to a very small tip [53]. The collision of primary electrons with the surface can be both elastic and inelastic. In an inelastic collision the outermost electrons, down to a depth of 10 nm, are removed from the sample and are transmitted as secondary electrons. These electrons are emitted out to the vacuum if an ionized atom on the surface does not capture them. The result is signal of secondary electrons, received by a detector, which represents a very small area of the sample. It's the secondary electrons that are used for production of high-resolution images. When the primary electrons reach the surface several other particles are also produced: backscattered electrons, auger electrons, x-rays and cathodoluminescence [54]. Detectors for secondary electrons are usually present in the setup, but there are seldom detectors for all different particles in the same machine.

3.10.2. Dynamic light scattering (DLS)

Dynamic light scattering technique is mostly used to measure the size of the colloidal particles in the solution. This technique is based on the Brownian motion of the particles. The equipment composes of a light laser that shines monochromatic light beam through the particles. The light wavelength change when it hits the spherical particles in Brownian motion due to Doppler Effect. The intensity of the scattered light fluctuates at a rate that is dependent upon the size of the particles as smaller particles are moved further by the solvent molecules and move more rapidly. Analysis of these intensity fluctuations gives the velocity of the Brownian motion and hence the particle size using the Stokes-Einstein relationship. This technique is very fast and easy to use as all the processes are automatized and extensive experiment is not needed. The theory of this technique is based on two assumptions. First it is needed to assume that the colloidal particles are in Brownian motion and in this situation we can calculate the diffusion coefficient (velocity of the Brownian motion). Second all particles are spherical with small diameter compare to the molecular dimensions that then it is possible to apply the Stoke-Einstein relation (2) to calculate the radius of the particles [55].

$$D=k_BT/3\pi\eta d(H) \qquad (2)$$

D: translational diffusion coefficient (velocity of the Brownian motion)
d(H): radius of the particles
k_B: Boltzmann constant,
T: temperature in kelvin degree
η: the viscosity of the solvent

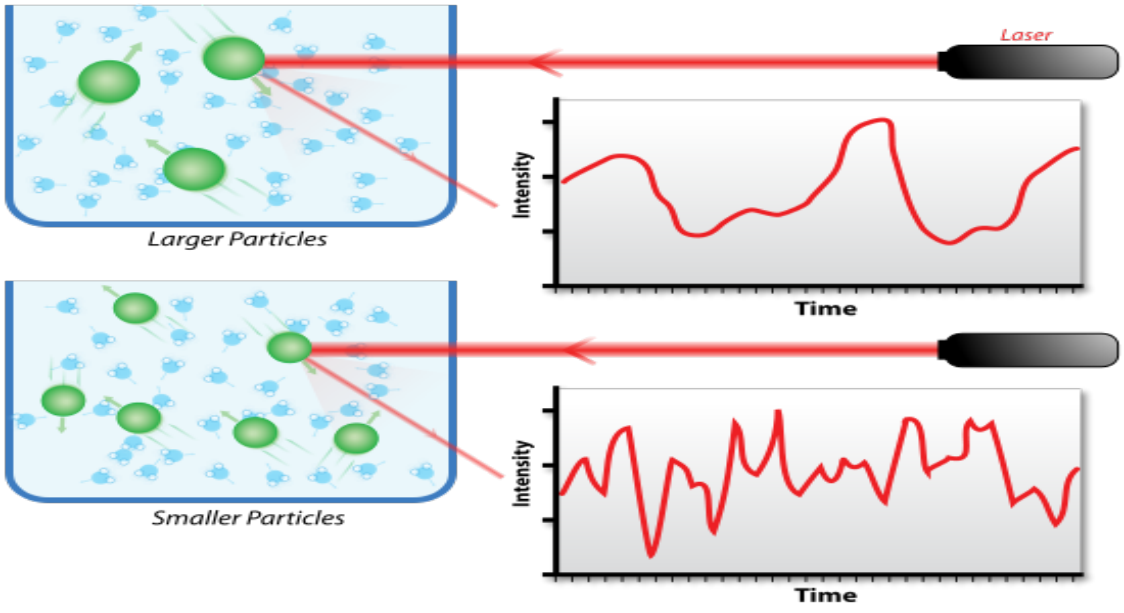

Fig 6. Dynamic light scattering of two samples: Larger particles on the top and smaller particle on the bottom. The laser light hits the particles and scatters and one observed a time-dependent fluctuation in the scattering intensity [56].

3.10.3. Spectrophotometer

Spectrophotometer was applied in this project to characterize the size of the particles in the solution and also to determine the concentration of bacterial solution. Spectrophotometer

composes of spectrometer and photometer in order to generate light and measure the intensity of light respectively. When the light generated by spectrometer passes through sample, sample absorbs some of the light and then the photometer measures the intensity of the light. This technique measures the amount of light absorbed by sample at appropriate wavelength and then it is possible to determine the concentration by the Beer–Lambert law, also known as Beer's law which is defined as below [57, 58]:

$$A=ebc \qquad (3)$$

Where A is absorbance ($A = log_{10} P_0 / P$, P_0: *the intensity of original light, P: the intensity of light after passing through the sample), e* is the molar absorbtivity, b is the path length of sample and c is the concentration of the compound in solution

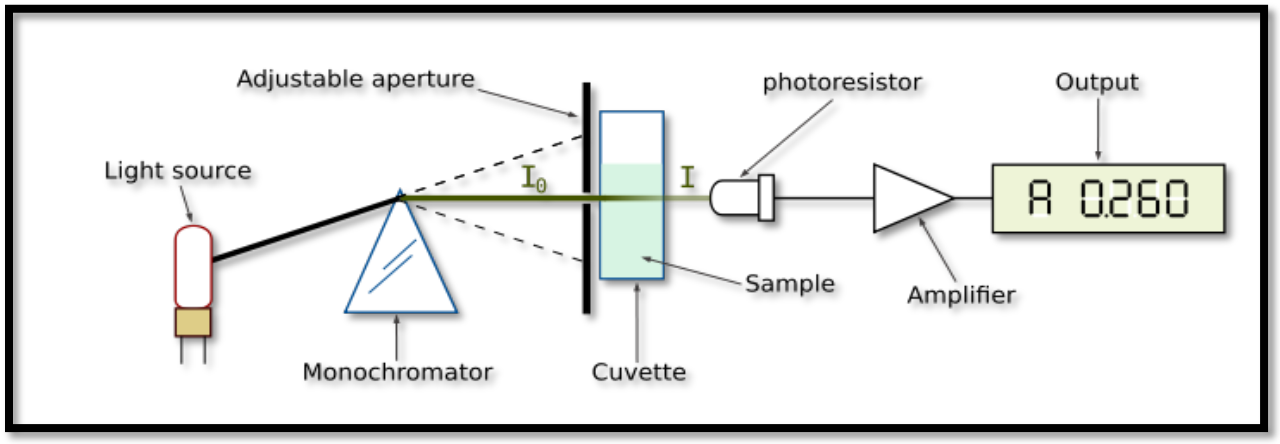

Fig 7. A scheme of spectrophotometer [59].

3.10.4. Contact angle

The contact angle, θ, is the angle formed between the solid and the tangent to the drop surface (fig. 8). A common method used to measure contact angle is optical tensiometry. The basics of this method are to analyze the shape of the test liquid drop on a specific surface. Low contact angle represents more hydrophilic surface [60].

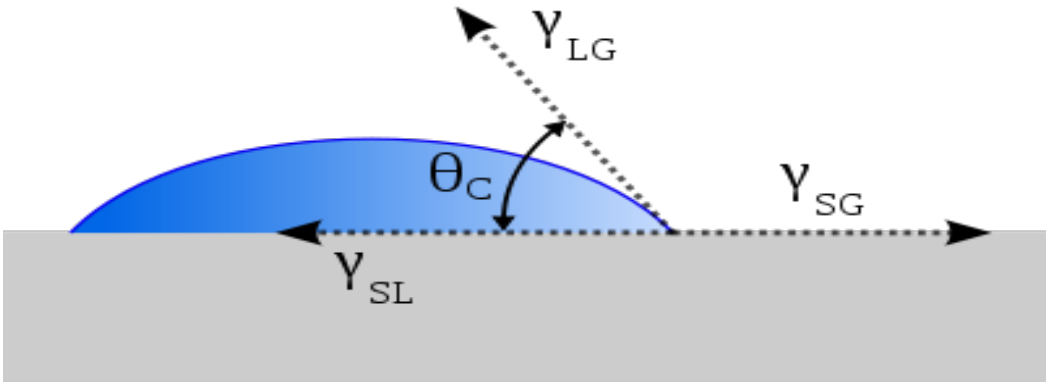

Fig 8. Illustration of a contact angle (θ_c) of a liquid sample [61].

3.11. Cell analyzing methods

To analyze if cells produce extracellular polymeric substances, fluorescence microscopy can be used. Fluorescence microscopy can also use for cell counting analysis.

3.11.1. Fluorescence microscopy

Fluorescence microscopy is used to observe cells or tissues that have been labeled or stained with one or more fluorescent probes. The samples can be viewed with two different types of light sources; normal light (halogen light) or fluorescence light (metal halite light). The normal light can be used to focus on the surface of the sample before the fluorescence light is turned on. This procedure is recommended to minimize photo bleaching the sample. This is especially important when weak fluorophores are used or when the amount of fluorophore is small [62].

In figure 9 an illustration of a typical microscope for fluorescence microscopy can be seen. The limitations of detection for these kinds of microscopes are normally dependent on the darkness of the background and the excitation light is often much brighter than the emitted fluorescence [62].

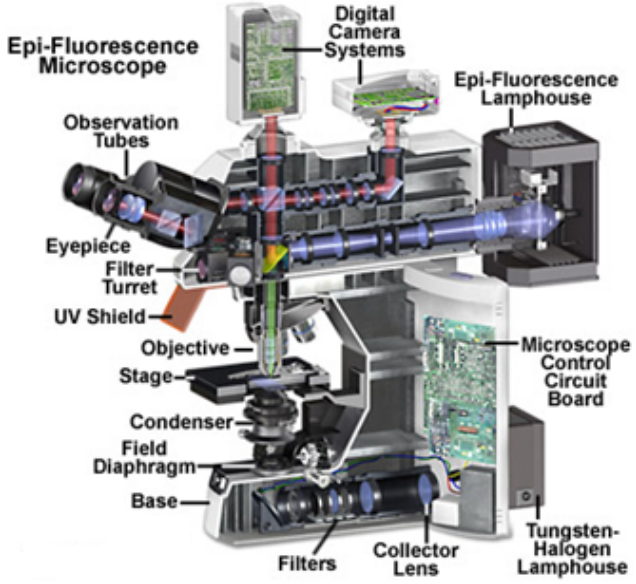

Figure 9. Illustration of a fluorescent microscope [62].

The microscope is used to illuminate the sample with a desired range of wavelength and then separates the emitted fluorescence from the excitation light. In front of the light source there is a filter that only lets the desired wavelength pass. A dichromatic mirror is also used in the setup that reflects light below a specific wavelength and let light pass that are above a specific wavelength. The dichromatic mirror reflects the light from the light source that illuminates the sample and the dye is excited and emits light at a different wavelength. The emitted light passes through the dichromatic mirror and the emission filter and hits the detector. Finally the image is visualized through the oculars [62].

3.11.2. Quartz Crystal Microbalance with Dissipation Monitoring (QCM-D)

Quartz Crystal Microbalance with Dissipation Monitoring (QCM-D) is a very sensitive and acoustic technique that is able to measure changes in the resonance frequency (Δf) of an oscillating sensor crystal, and in dissipation (ΔD) of an adhering mass on a quartz-crystal

surface. With these measurements both the amount and viscoelastic properties of the adhering mass are determined [63-65].

Quart is a material with a very unique property named piezoelectricity. Piezoelectricity is the charge that accumulates in the material as a result of mechanical stress and was observed first by Jacques and Pierre Curie. Shortly after that, it was discovered that an electric potential around the crystal can cause mechanical strain and it was named converse piezoelectric effect. This phenomenon is the base for QCM-D measurements. A QCM sensor composes of an AT-cut piezoelectric quartz crystal that has been surrounded with two metal electrodes that are applied to make an electric field around the crystal. Once appropriate AC voltage is applied across these electrodes, the crystal oscillates at its overtones and at its resonant frequencies. According to the changes of amount of the mass adhered on the surface of the crystal, frequency changes. These changes in frequency can be used to calculate the mass adsorbed on the surface using the Sauerbrey equation [66, 67].

$\Delta f/f_0 = -\Delta m/m$ (4)

$\Delta m = - C \cdot \Delta f/z$ (5)

Where C = 17, 7 ng/ (cm Hz) is the resolution for a 5 MHz crystal and z is overtone number.

The results achieved from Sauerbrey equation are reliable when it assumes that the adhered layer is part of crystal itself. The attached layer needs to have three conditions in order to make this assumption true: 1) it should be small compare to the mass of the crystal, 2) attaches on the surface rigidly, 3) and distributes over the crystal evenly [68, 69].

Based on Sauerbrey theory the frequency shift should be negative once colloidal particles attach on the surface. However, positive frequency shift has been observed for various types of colloidal particles such as bacterial cells and diatoms [70-72]. This phenomenon cannot be explained by mass-loading theory. Positive frequency shift can be explained as another theory named coupled-oscillator theory. Based on this theory magnitude of adhered mass and stiffness of the bond between the adsorbed mass and crystal sensor- surface affect the frequency through the equation below (equation 6) [70]:

$$2(2\pi f)^2 = \left(\frac{K}{M} + \frac{k}{M} + \frac{k}{m}\right) \pm \sqrt{\left(\frac{K}{M} + \frac{k}{M} + \frac{k}{m}\right)^2 - 4\frac{K}{M} \times \frac{k}{m}} \quad (6)$$

f: the resonance frequency of the quartz-crystal sensor

K: the spring constant

k: spring constant describing the stiffness of the particle sensor contact point

M: the mass of the quartz-crystal sensor surface

m: the mass of the adhering particle

Based on the equation 6 the resonance frequency of coupled-oscillator can be affected by spring constant (k) that relates to contact point stiffness. Basically put less stiff contact lead to small k-values and consequently lead to positive frequency shift that increase non-linearly with stiffness.

While large k-value is achieved by stiffer contact points which lead to negative frequency shift. A combination of these two theories coupled-oscillator and normal mass-loading theory are required to be able interpretation of QCM-frequency shifts in bacterial adhesion properly [70].

The dissipation can describe the molecular organization and conformation of the adhered material. If the adhere layer become viscoelastic, there will be a loss of energy due to internal friction in the film. The higher value of the dissipation leads to the higher energy loss. Dissipation is calculated with the following equation:

D= 1/Q factor (7)

Q factor= 2π E1/E2 (8)

E1: the total energy stored in the oscillator

E2: the energy lost (dissipated) during one oscillation cycle

The Q-factor represents the amount of energy stored between the oscillation cycles. Since dissipation is the inverse of Q-factor, high loss of energy represents low value of Q-factor and consequently high value of dissipation. In order to measure the dissipation of the crystal, response of a freely oscillating crystal that has been vibrated at its frequency is recorded. With the use of viscoelastic model (Voigt model), measurements at multiple frequencies and Q-sense software named Q-tools the characteristic of attached layer can be determined in detail [73].

4. Materials and methods

4.1. Preparation of gold nanoparticles

In order to prepare gold nanoparticles, Turkevich method was utilized. At the first step 0.295 ml of %1mM $HAuCl_4$ aqueous solution was added to 47.5 ml water and then the solution was heated to 100 °C while stirring continuously. In the next step, 2 ml of 1% w/v sodium citrate was added quickly. After the addition of sodium citrate, the color of the originally yellow solution changed to dark blue but then it changed to red. The solution was heated at 100 °C for 15 min while stirring constantly. The final size of the particles was then estimated by using Dynamic Light Scattering, Spectrophotometer and Scanning Electron Microscopy techniques. After the preparation of nanoparticles, Dynamic Light Scattering (DLS) was run once to determine the size of the particles. In addition to above technique, spectrophotometry also was used to estimate the size of the particles. According to the study has been done by W. Haiss, it is possible to determine the size of the particles from UV-Vis spectra. Gold nanoparticles have an absorption peak around 510- 550 nm in the visible range [74].

4.2. Preparation of nanostructured surfaces

Gold substrates were purchased from Litcon AB, Sweden. The substrates were prepared on 8x8x0.5mm silica wafers by RF sputtering of 150 nm gold on a supporting layer of 8 nm of titanium. The mean surface roughness (Rms) of the gold substrates was 0.9 nm according to atomic force microscopy (AFM) measurements from the manufacturer. All gold surfaces were first placed in UV/OZON oven for 30 minutes to be cleaned. Then gold surfaces ere washed for 10 minutes at 70-80º C in a basic piranha solution containing (Milli Q water, 15 ml; Ammonia (25%), 5 ml; Hydrogen peroxide (30%), 5ml), washed in excess of Milli-Q water and dried in

gaseous N_2. Quartz crystal (Gold plated Sensor Crystal, Qsense, Sweden) was washed with the same procedure mentioned above. Completely cleaned surface was placed in 25 ml of 20 mM cysteamine for 6 hours in order to chemically modify the surface. The cyteamine will attach on the surface from its thiol group and its amino group attach to nanoparticles. After 6 hours surfaces were washed carefully first with ethanol and then with Milli-Q water. Finally, the surface was placed in 1 ml particle solution for 15 hours.

All surfaces were washed again before the experiment in order to melt down the nanoparticles on the surface and to be sure that the nanoparticles are immobilized on the surface. Since nanoparticles have attached on the surface via electrostatic attraction it is possible that they move on the surface during the experiment. Therefore by melting down the particles on the surface there will be no motility during the experiment. Moreover washing the surfaces in piranha solution will wash away any residue of cysteamine.

In this project the effect of different ion strengths (I= 23.22, 11.58 and 5.76) were also investigated in order to show how particle coverage changes with changes in ionic strength of the particle solution. Ionic strength equal to 23.22 was the ionic strength of particle solution but for reducing ionic strength to 11.58 and 5.76, 0.5 ml and 0.25 ml of particle solution were diluted with 0.5 ml and 0.75 ml Milli-Q water respectively. One surface was kept in each solution with different ionic strength and 5 images of each surface were analyzed in order to calculate the particle coverage.

4.3. Surface characterization

SEM (Zeiss 982 Gemini Scanning Electron Microscope) was utilized to measure the particle size and particle coverage on the surface. 10 images with 50000X magnification were captured from three different surfaces and were analyzed using the software imageJ. In order to count the particles on each surface, a threshold value is chosen to distinguish light objects (particles) from the dark background. The program then marks everything that will be counted as particle. After the threshold is set, the program will count the white marks in the picture. Then the function analyze particles is used where the size range can be set as well. This is useful for excluding small particles and noise that are too small to be a particle but to light to be excluded by the threshold value. After the function is used, the results are presented in table with the number of particles and also area fraction that represents the particles coverage. The particle coverage was evaluated for all 10 images of three different surfaces. In order to compare the particle coverage on the surfaces that were kept in particle solution with different ionic strength, 5 images from each surface were evaluated.

After the threshold is set, all the pixels relate to all the particles can be achieved through the histogram form the image. By having the number of particles, it is possible to calculate the number of pixels per particle. In the next step by setting the scale and finding out that how many pixels represent one nm, it is possible to calculate the diameter of particles. These calculations were done on 5 images of three surfaces.

The hydrophobicity of the surfaces was determined by measuring the water contact angle. Three measurements were done on one flat and one nanostructured surface. The measurements were done immediately after the washing procedure.

4.4. Bacterial strain and culture condition

S. epidermidis ATCC 35984 were cultivated in 5 ml Luria broth (LB: tryptone, 10g; yeast extract, 5 g; NaCl, 5 g; Milli Q water, 1000ml; pH 7.3)at 37ºC with shaking overnight. Cells were then harvested three times by centrifugation and washed with 15 ml of PBS (NaCL 8.5 g; Na2HPO4, 1.34 g; NaH2PO4 · 2H2O, 0.39 g; Milli Q water, 1000 ml; buffered to pH 7.3 with NaOH). Cells were then suspended and stored in 5 ml PBS overnight. Following day cells were twice harvested by centrifugation and washed in PBS. Thereafter, right before usage, the cell suspension was diluted with PBS to the desired concentration (OD: 0.75).

4.5. Determination of bacteria concentration

Bacterial concentrations were determined by a spectrophotometer at wavelength 600 (model; Ultraspec 2000 UV/Visible spectrophotometer (Amersham Pharmacia Biotich)). To avoid errors regarding concentration, caused by differences between spectrophotometer, the same one was used during the entire experimental period. The desired OD was between 0.7 and 0.8.

4.7. Scanning electron microscopy

Scanning electron microscopy (Zeiss 982 Gemini Scanning Electron Microscope) was used to compare the number of cells attach on surfaces and also to analyze the morphology of bacterial cell. Before running the SEM experiment one QCM-D measurement was performed in order to find the critical incubation times and according to QCM-D graph the best critical time point were 0.5, 2.5, 5, and 7.5 hours. The bacterial solution was incubated for four time points (0.5, 2.5, 5 and 7.5 hours). Then the surfaces were kept in Glutaraldehyde solution for 20 minutes in order to fix the bacteria on the surface. Surfaces were then pre-fixed with karnowsky solution and then were washed with 0.15 M Na-kakodylat. In the next step they were post fixed with 1% OsO4 and 10M Na-kakodylat twice at 4 ºC and then washed 5 times with milliQ water. Then they were kept in 1% thiocarbohydrazide (TCL) for 10 minutes at room temperature and washed with milliQ water 5 times. In the following step all surfaces were kept in 1% osmiumtetroxide solution for 1hour at 4 ºC and then washed twice with milliQ water. Finally they were dehydrated in an ethanol-milliQ water series (70%, 85%, 95%, and 99.5 % ethanol), for 10 minutes each. This was followed by exposure to hexamethyldisilazane (HMSD)-ethanol series (50% and 100% HMSD), for 10 minutes each. The samples were then left to dry overnight and became ready to analyze with SEM. SEM images were then applied to compare the number of cells attach on surfaces and also to analyze the morphology of bacterial cell. For each time point one surface were analyzed. 23% of each surface was evaluated in order to count the number of cells attached on the surface.

Anova (single factor) was applied as analysis tools and the confidence interval of 95% has been chosen and P value lower than 0.05 was considered significant. N represents the number of measurements.

4.8. Fluorescence microscopy

The flat and nanostructured surfaces were kept in bacterial solution for three different time points (0.5, 2.5 and 5 hours) and then were stained by FilmTracer TM SYPRO Ruby biofilm matrix stain. For each time point one surface was analyzed.

Biofilm were stained with an EPS specific fluorescent dye (film tracer SYPRO Ruby biofilm matrix stain, Invitrogen), and visualized by fluorescence microscopy. At first 200 μL of

FilmTracer™ SYPRO® Ruby biofilm matrix stain was added onto the biofilm sample. The addition was done very slowly to prevent disturbing of the biofilm. In the next step the sample was kept for 30 minutes at room temperature and protected from light. After 30 minutes it was washed with water very gently and then visualized by fluorescence microscopy.

Thirty images were captured with 100X magnification in order to cover 27% of the each surface and the exposure time and aperture were the same for all images (exposure time=50 ms). The images were then evaluated by imageJ software. The red spot on each image represents extracellular polymeric substances (EPS). The histogram of each image shows that at different intensities (from 0(intense red) to 225(black)) how many pixels exist. Then the program imageJ calculate the integrated intensity for all intensities. Integrated intensity is the multiplied of intensity and the number of pixels exist at that intensity. The summation of all integrated intensities represents the amount of EPS. These calculations were done on all thirty images and the mean values show the amount of EPS produced at each time point for flat and nanostructured surfaces. One program was design to perform all the steps in imagej (appendix).

4.9. QCM-D experiments

A QCM-D instrument (model; D300 (Qsense, Sweden)) was first calibrated with the same PBS buffer solution used to wash bacterial solution. The experiment was run at the same time for flat and nanostructured surfaces and the same bacterial solution were used for both surfaces. When frequency drift was less than 2 Hz over a period of five minutes it was considered stable and 1.5 ml of the bacterial solution was added. The condition that was considered stable in this project is not very good because the QCM-D instrument used was very old and it was hard to achieve a completely stable condition. Software Q-Tools was used to analyze the data provided from experiment. The experiments were run overnight. The temperature was kept constant for all the experiments and it was around 22 ºC. Since the equipment was very old it was not possible to keep the temperature stable in a case of high temperature and because of that 22 ºC was chosen. All data of QCM-D represented in this report were normalized against their respective overtone. This experiment was run three times and all the results were analyzed.

5. Results

5.1. Characterization of the surface

Several techniques were applied to determine the size of the particles on the surface and also the particles coverage.

5.1.1. Dynamic light scattering

This technique was applied to measure the size of the colloidal particles in the solution. As shown in graph 10 the average particle size was 24 nm and the overall size distribution ranged from around 10 to 60 nm.

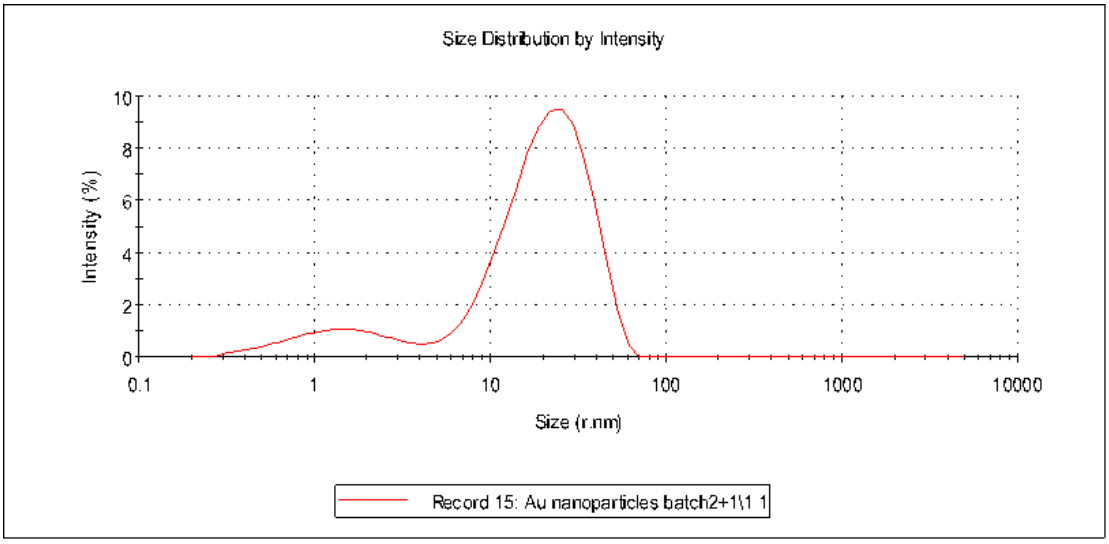

Figure 10. Graph of Dynamic Light Scattering showing the size distribution of the particles.

5.1.2. Spectrophotometry

In addition to above technique, spectrophotometry was applied to measure the size of the particles. The result revealed that the peak is at wavelength 518 that indicates that the size of the particles is around 20 to 25 nm [74].

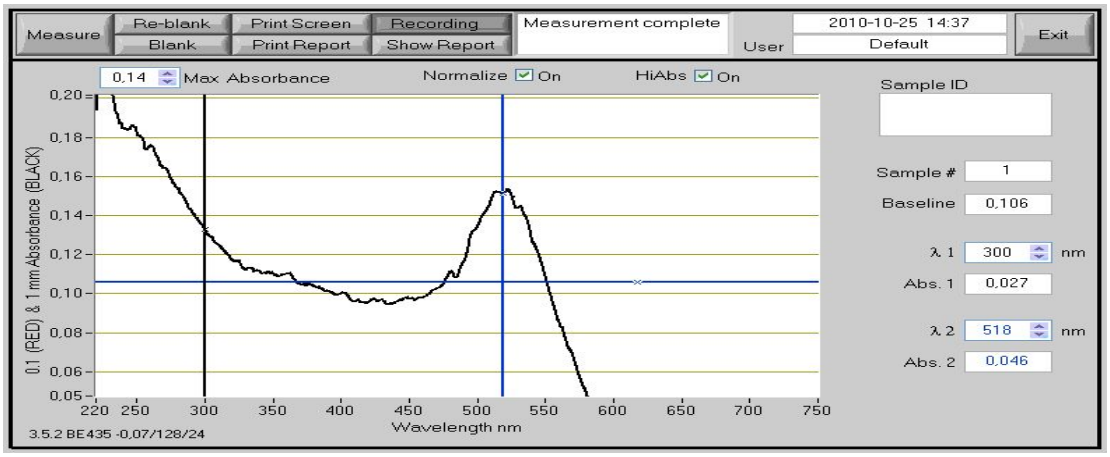

Figure 11. Absorption spectrum of gold NP solution. The peak at 518 nm represents a particle size of 20-25 nm.

5.1.3. Scanning electron microscopy

The images provided by scanning electron microscopy show that the size of particles was 18±3 nm, and covered 23% (SD=0.42) of the surface.

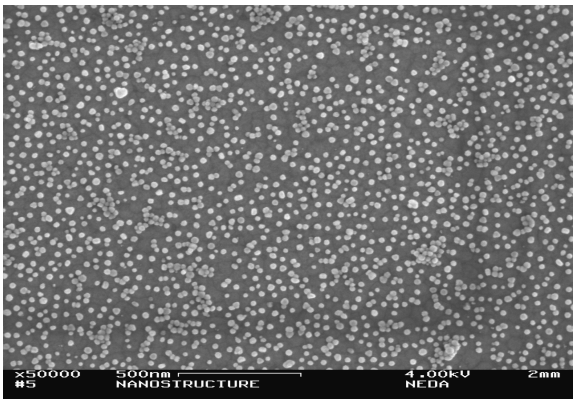

Figure 12. SEM images show particle distribution on the surface.

As it has been shown in fig13, low ionic strength of the solution results in less aggregation and also lower particle coverage. According to calculation, particle solution with I=23.22 gives particle coverage equal to 23%(SD=0.42) while for two other particle solution with I=11.58 and I=5.76 the particle coverage is 12%(SD=0.61) and 7% (SD=0.56) respectively. Since in this project having high particle coverage was the aim it was tried to have reasonable particle coverage with low aggregation.

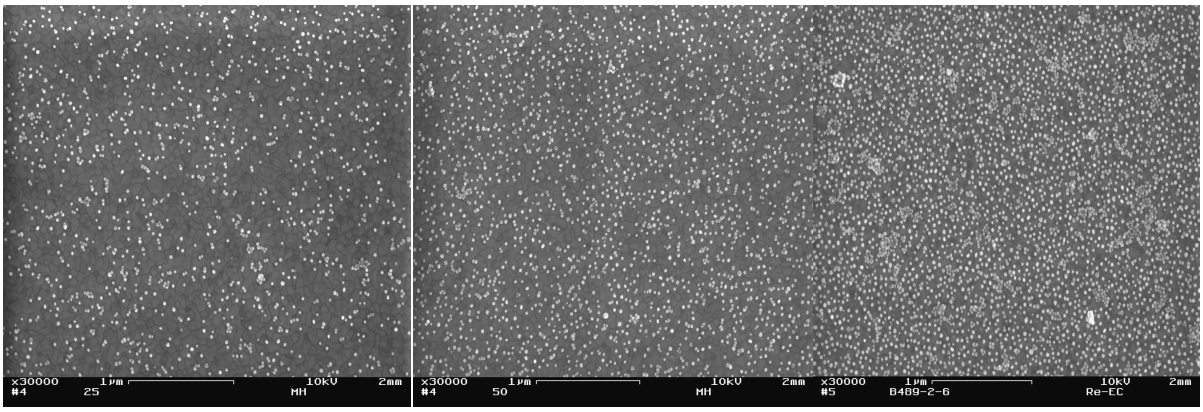

Fig 13. SEM images show the effect of increase in ion strength of particle solution from left to right (I= 23.22 (a), 11.58 (b) and 5.76 (c)) on particle coverage. In high ionic strength the particles come closer while in low ionic strength particles are more separated.

5.1.4. Contact angle

Hydrophobicity of the flat and nanostructured surfaces was compared by measuring the contact angle. Figure 14 shows that the structured surface has lower contact angle around 8° (SD= 0.16), and the flat surface has a contact angle around 12° (SD=0.083) that indicates flat surface it less hydrophilic compared to the structured surface. (N=3, P= 0.003)

Although there is a significant difference in contact angle between flat and nanostructured surfaces, the difference is very small and this means that the surface chemistry is essentially similar.

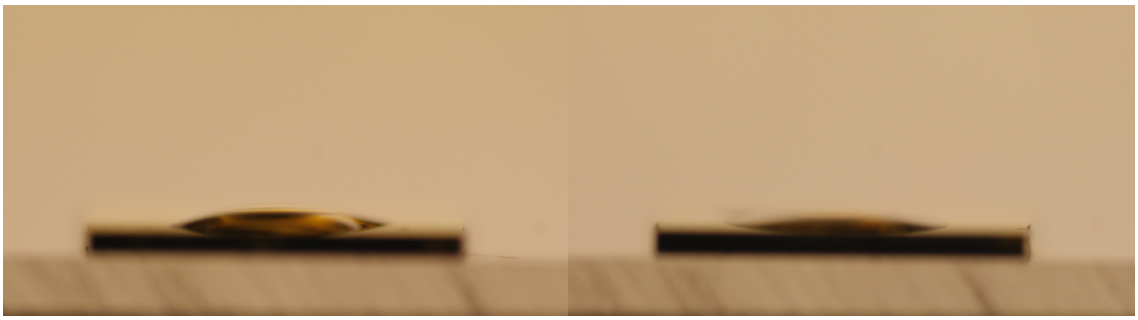

Figure 14. Contact angle measurements. Left: flat. Right: structured.

Table 1 displays the measured values of flat and nanostructured surfaces.

Table1. Contact angle measurements

Contact angle measurements of flat surface	Contact angle measurements of nanostructured surface
12.6°	7.92°
11.91°	8.16°
12.05°	8.23°

5.2. Cell observation

5.2.1. Scanning electron microscopy

The results show that the number of cells attached on both surfaces at each time point is the same. (N= 15, P-value= 0,991)

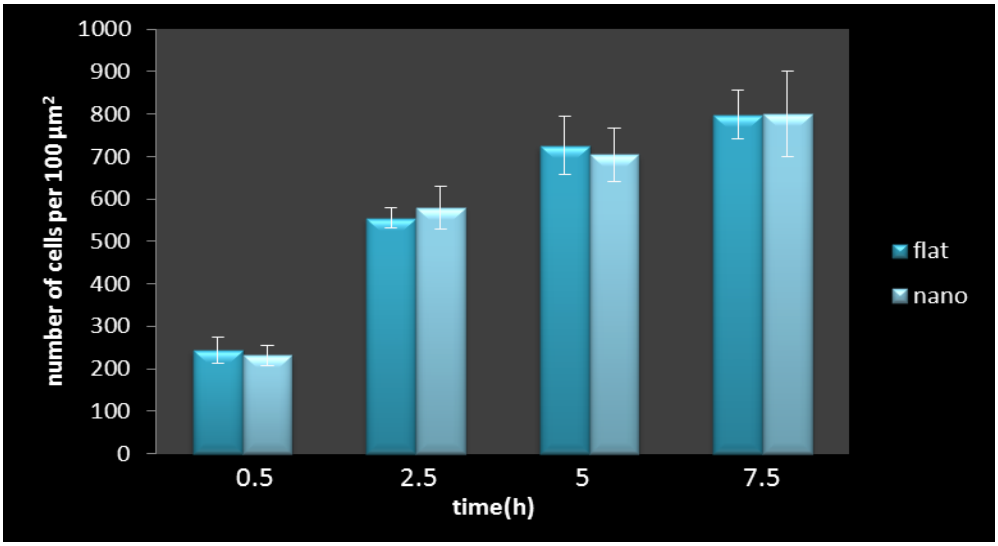

Figure 15. Results obtained from SEM images to show the number of cells attaches on the flat and nanostructured surfaces. The error bars represent the standard deviation. (N= 15, p= 0,991)

SEM images show that not only there were more bacteria on the surface with time but also there were more accumulation of bacterial cells and production of EPS on both flat and nanostructured surfaces with time (fig 16, fig 17).

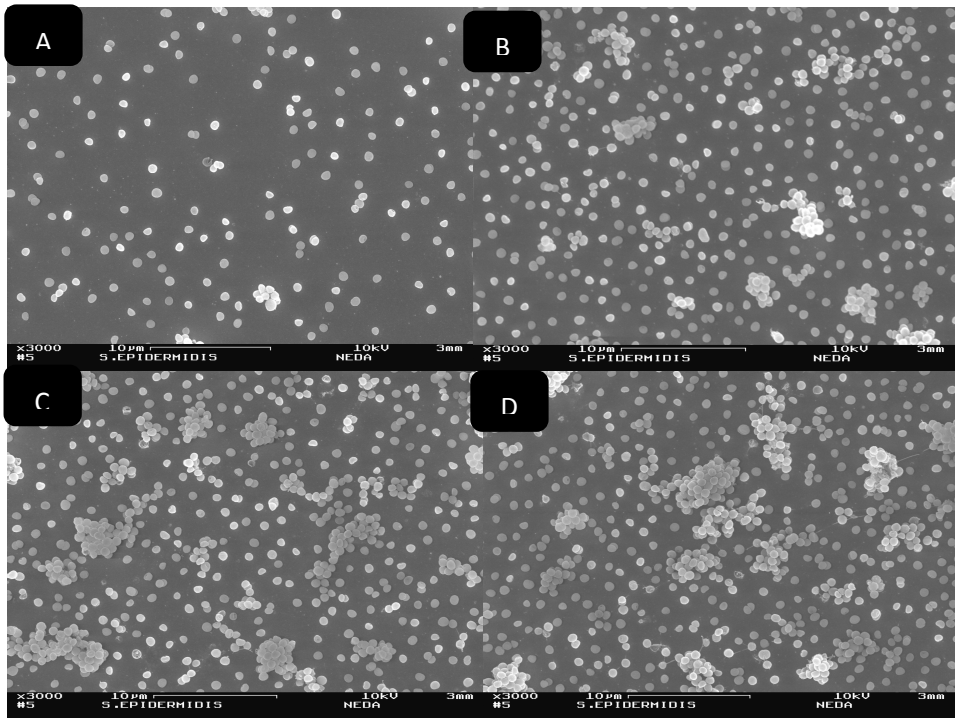

Figure 16. SEM images show the number of bacterial cells attached on flat surface in different incubation time 0.5 (A), 2.5 (B), 5 (B) and 7.5 (D) hours. These images show that the number of bacterial cells attached on flat surface increases with time.

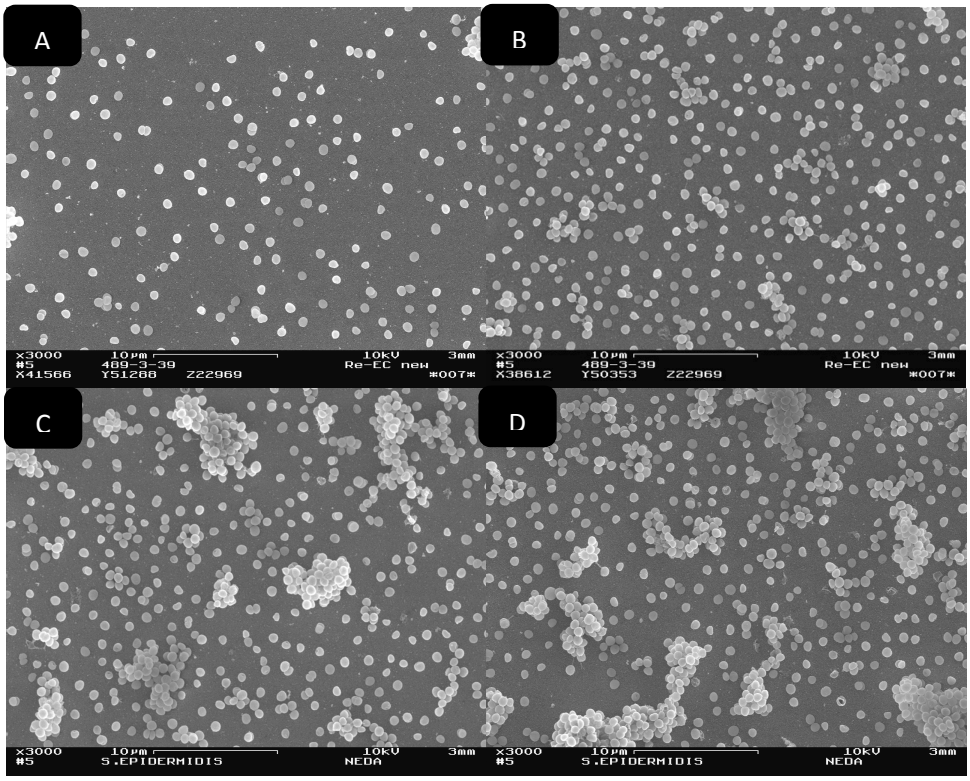

Figure 17. SEM images show the number of bacterial cells attached on nanostructured surface in different incubation time 0.5 (A), 2.5 (B), 5 (B) and 7.5 (D) hours. These images show that the number of bacterial cells attached on nanostructured surface increases with time.

It was also observed that the number of cells attached on both surfaces increased significantly at the early stage of experiment while it slowed down with time (fig.18).

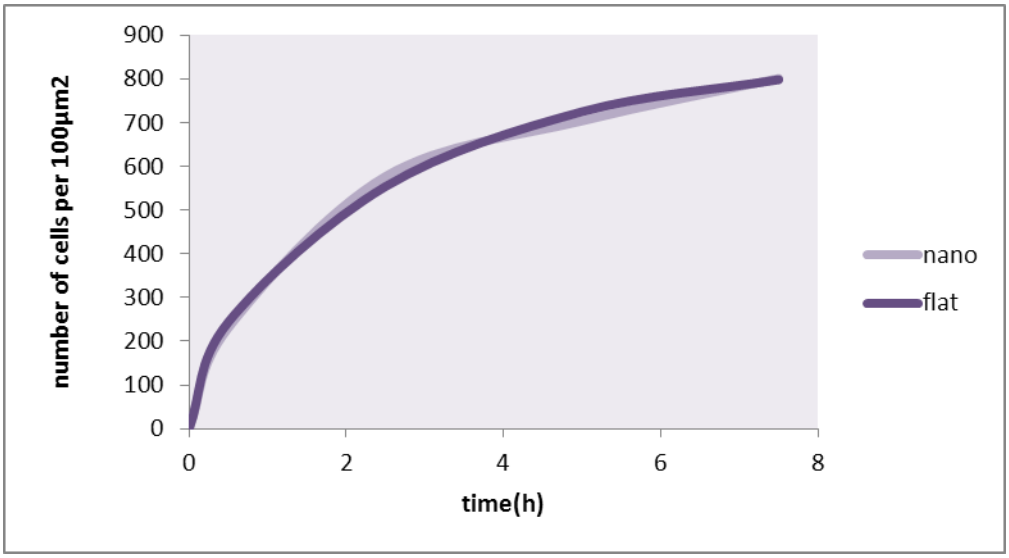

Figure 18. Graph representing the number of cells attach on flat and nanostructured surfaces with time.

SEM images of attachment of bacteria on flat surfaces after 2.5 hours show that bacterial cells have attached more firmly and have produced EPS.

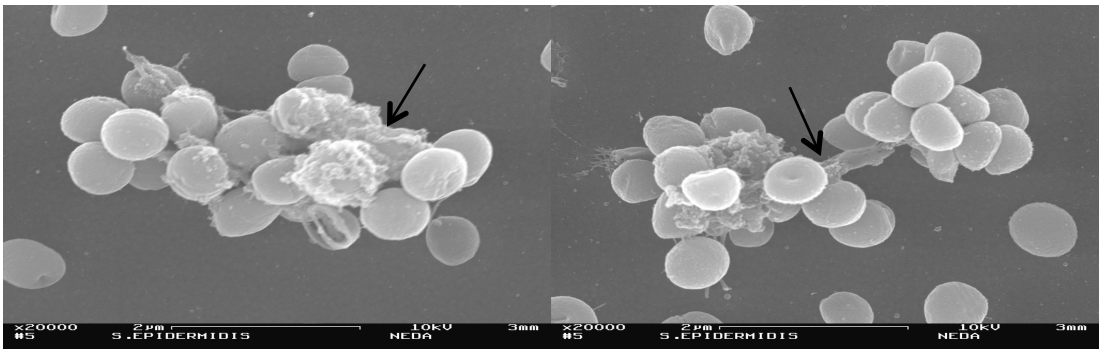

Figure 19. SEM images show production of EPS on the flat surface after 2.5 hours.

From the SEM images of attachment of bacteria on both flat and nanostructured surface, it seems that bacterial cells have behaved differently between flat and nanostructured surface.

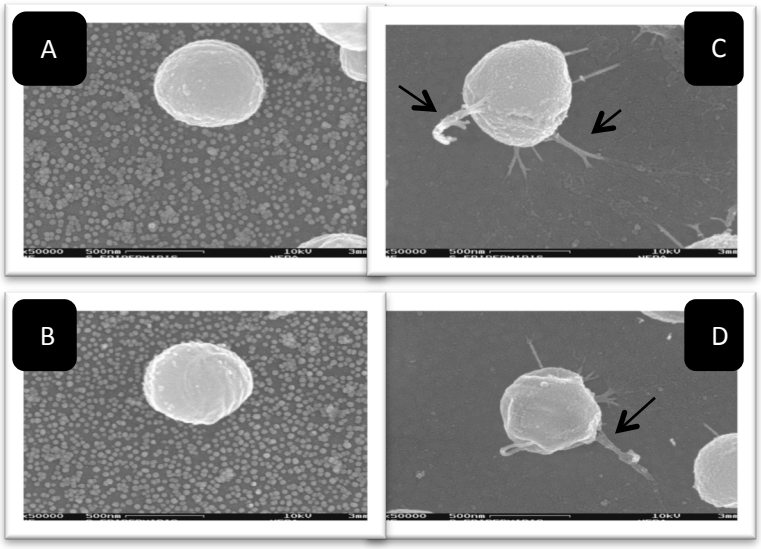

Figure 20. SEM images from surfaces indicate different behavior of bacterial cells on flat surface (A, B) compare to nanostructured surface (D, C) after 7 hours.

5.2.2. Fluorescence microscopy

The EPS formation on flat and nanostructured surface was shown in figure 21 and these images clearly illustrate that amount of EPS formed on both flat and nanostructured surfaces increased with time.

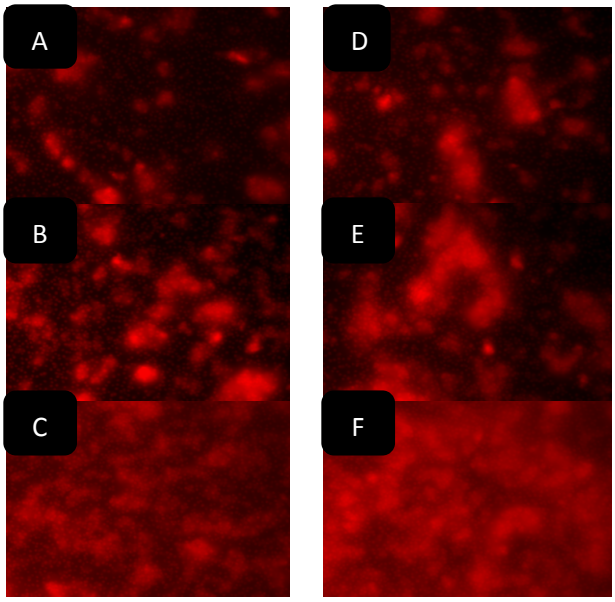

Figure 21. Illustration of formation of biofilm on nanostructured surface at different incubation time A) 0.5 B) 2.5 C) 5 hours and on flat surface at different incubation time D) 0.5 E) 2.5 F) 5 hours.

The graph in Figure 22 shows the amount of EPS produced by bacterial cells on flat and nanostructured surfaces at each time point. Based on this data the longer the surfaces were kept in bacterial solution the more EPS were produced on both surfaces. Based on this graph, the amount of EPS has produced on both surfaces is the same at each time point. (N=30, P = 0,488)

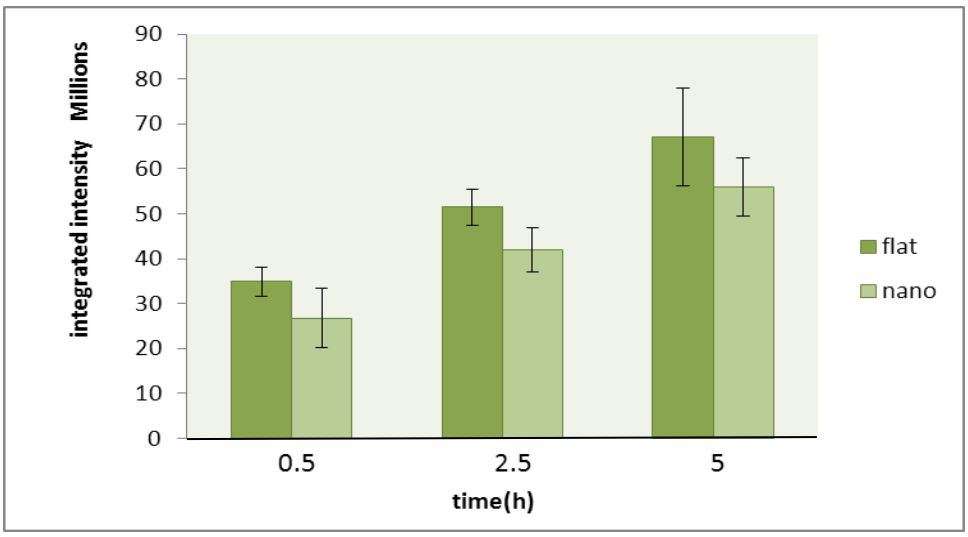

Figure 22. This graph shows the integrated fluorescence intensity on flat and nanostructured surfaces at different incubation time. The error bars represent the standard deviation. (N=30, P = 0,488)

5.2.3. Quartz Crystal Microbalance with Dissipation Monitoring (QCM-D)

The results show that there is a positive frequency shift in third overtone during 150 first minutes for flat surface but not for nanostructured (fig. 23). Moreover, for fifth and seventh overtones the

way the frequency has changed for both surfaces is similar and final frequencies are the same between both surfaces (fig. 23). The dissipation at the early stage of experiment (10 min) is quite the same for both surfaces but after that time is always higher on flat surface compare to nanostructured (fig. 24). Positive dissipation shift was observed from the beginning of the experiment as expected. The dissipation increases considerably at the early stage of the experiment, while with time it reaches the saturation level and keeps constant. (All the results are provided in appendix)

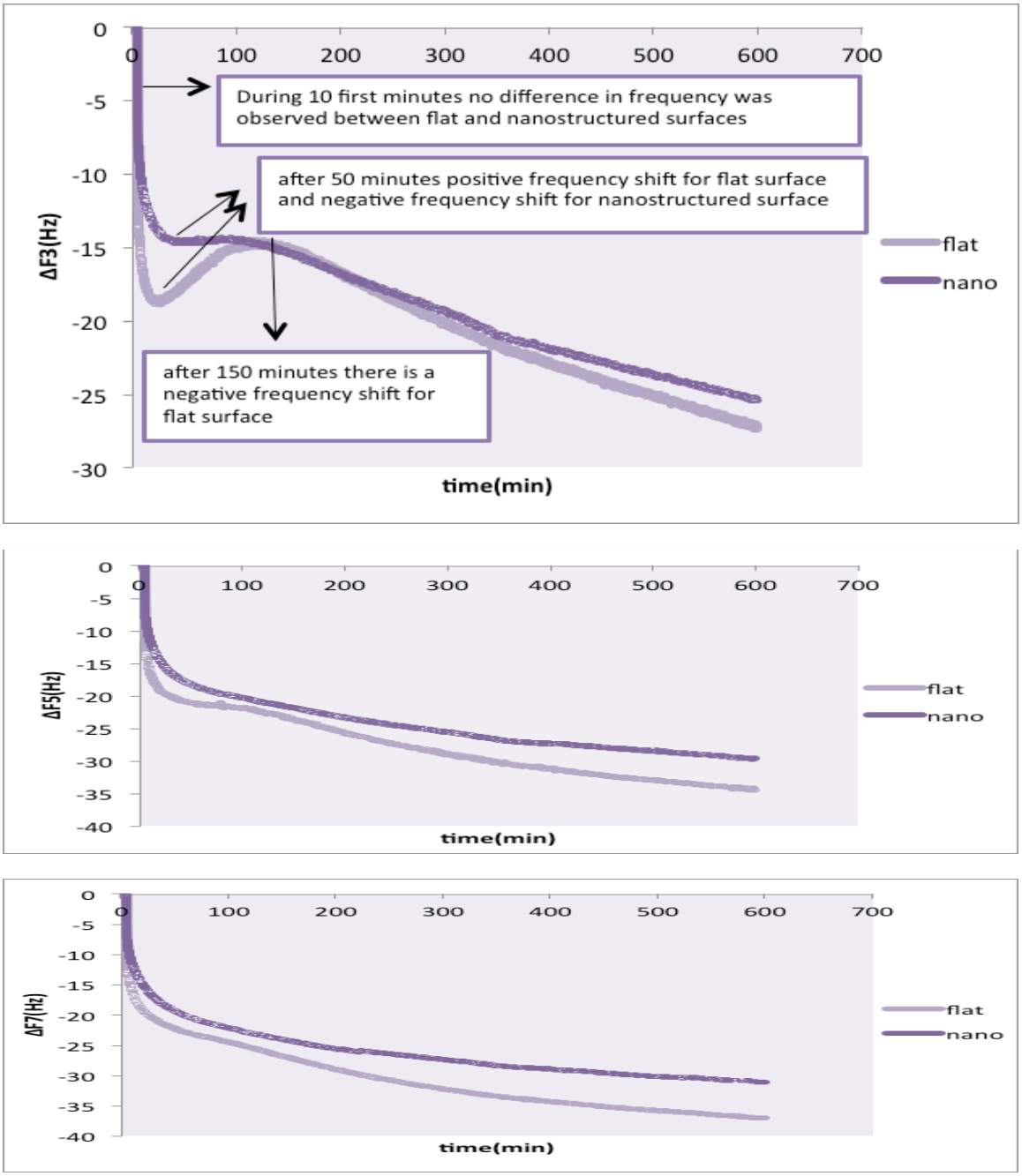

Figure 23. These graphs show the changes in frequency after the adhesion of bacteria on flat and nanostructured surfaces in third (A), fifth (B) and seventh (C) overtones. There is negative frequency shift on nanostructured surface on all overtones while for flat surface a positive frequency shift was observed in first 50 minutes of the experiment in third overtone.

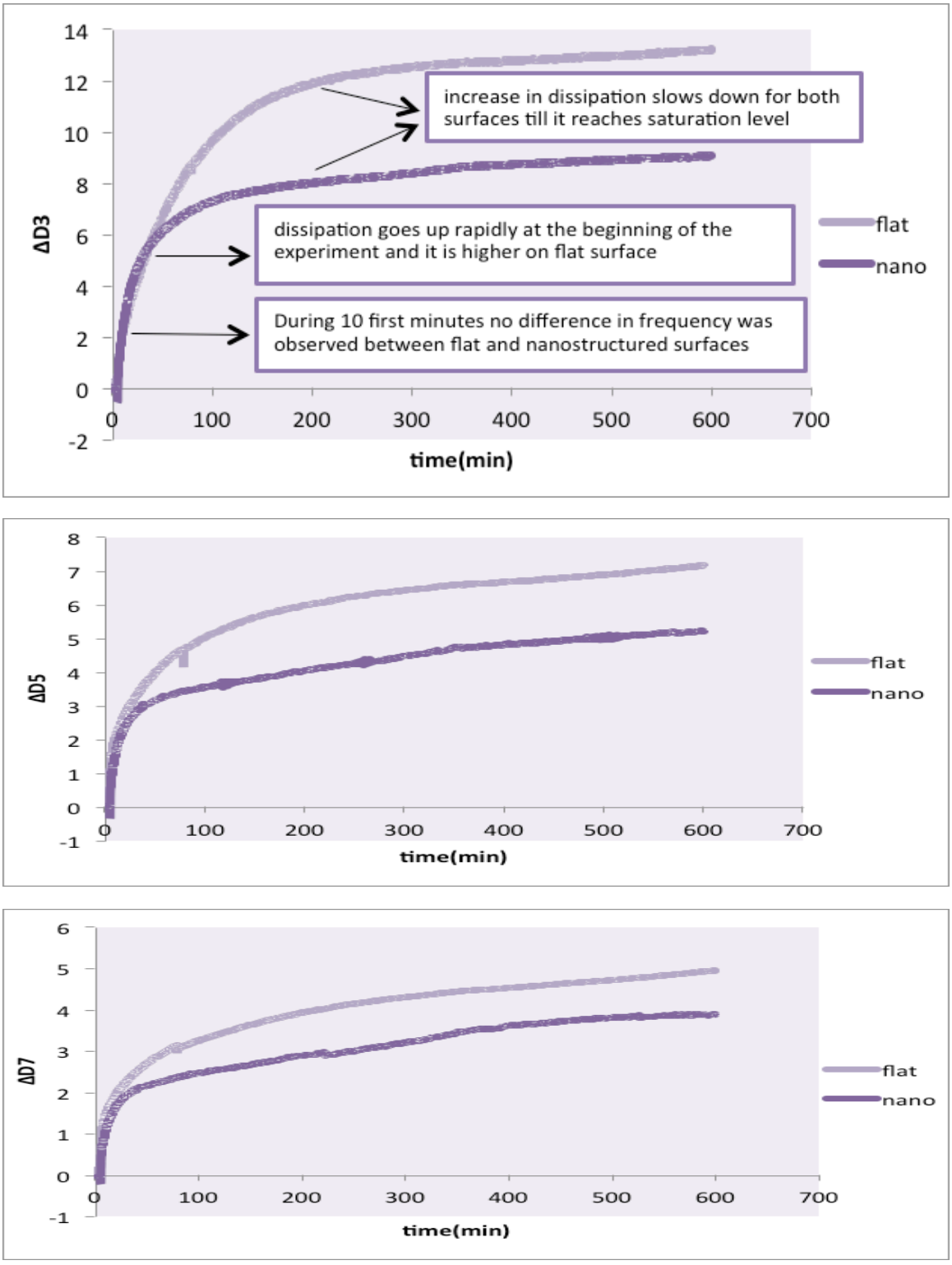

Figure 24. These graphs show the changes in dissipation after the adhesion of bacteria on flat and nanostructured surfaces in third (A) fifth (B) and seventh (C) overtones. Dissipation increased with time on both flat and nanostructured surfaces in all overtones and it is higher on flat surface.

There was a sharp decrease in frequency at the very early stage of the experiment for all three measurements on flat and nanostructured surfaces. In order to see if this decrease is due to protein adsorption on the surface one more experiment was performed. In this experiment the bacterial solution was centrifuge and solution above the bacteria was added to the QCM-D and the experiment was run for 20 minutes. The result shows that there is negative frequency shift in all three overtones and the adsorb layer is rigid because the changes in dissipation is low (fig 25).

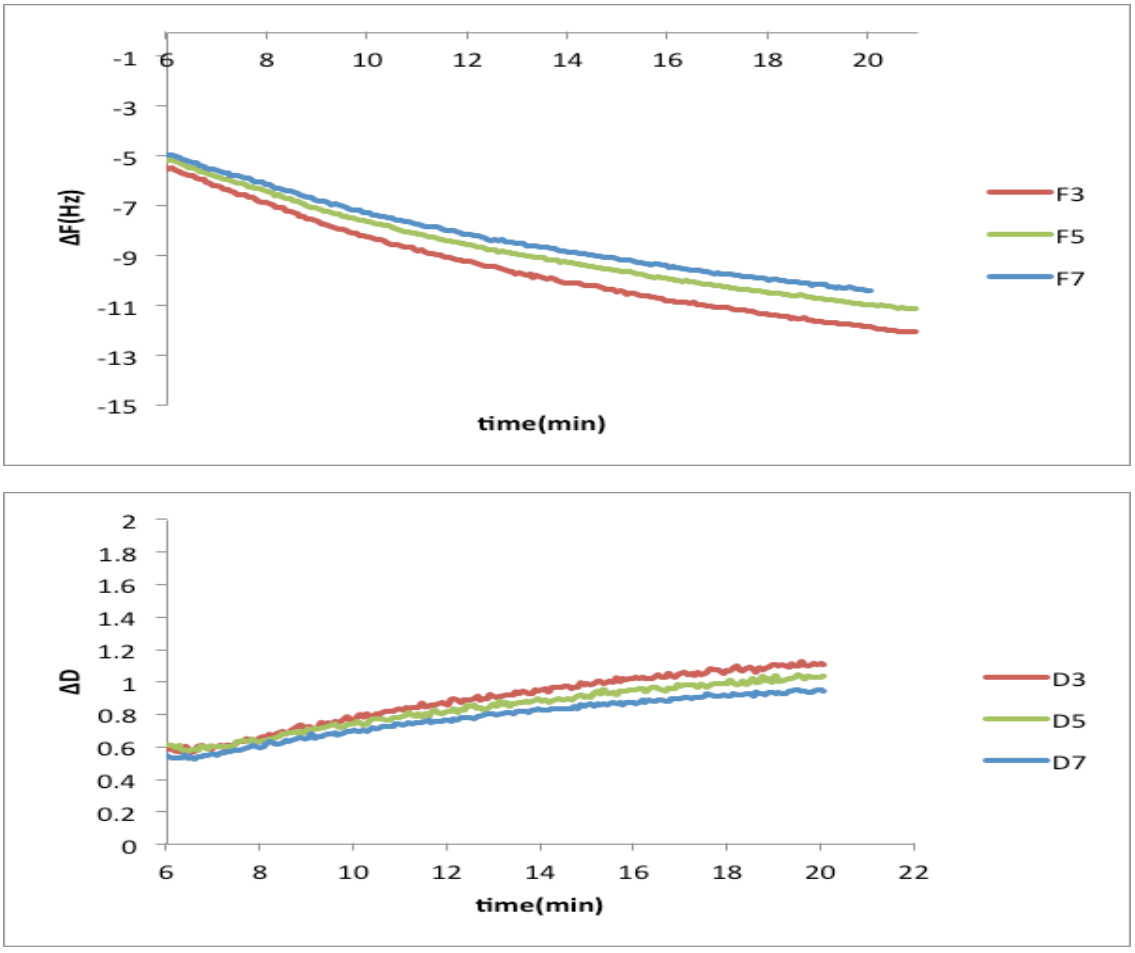

Figure 25. Adsorption of proteins present in bacterial solution on flat surface result in negative frequency shift and positive dissipation shift.

6. Discussion

6.1. Nanostructured gold surfaces

Small difference in water contact angles was found between flat and nanostructured surfaces. Based on the theory introduced by Wenzel, this difference in contact angle is due to nano-roughness [37]. Although there is a significant difference in contact angle between flat and nanostructured surfaces, the difference is very small and this means that the surface chemistry is essentially similar.

On all the surfaces provided with different ionic strength of the solution, there were some aggregations (fig.13). A probable explanation to this could be that the Milli-Q water in the laboratory was not clean enough, i.e. there were some ions left in it. Since the method has been used in this project is dependent on electrostatic repulsion between particles, for an even distribution of particles on the surface, any ions would interrupt this repulsion and thereby the even particle distribution. There could also have been some other contamination from the materials used during the surface preparation. For future experiments, all surfaces should be prepared in a cleanroom environment to ensure good quality.

Moreover, it was observed that particle coverage increased when ionic strength of the solution enhanced (fig. 13). The reason is that electric double layer that is formed around particles is bigger in solution with low ionic strength and each particle occupies larger space on the surface. While in the solution with high ionic strength the electric double layer is very dense and let the particles to be very close. In solution with very high ionic strength there is high chance of particle aggregation.

6.2. Scanning electron microscopy (SEM)

In this study, the result from SEM showed that nanotopography has no effect on the number of bacterial cells attached on the surface. Similar results have been seen by Campoccia et al. on the adhesion of *Staphylococcus aureus* on structured and reference surfaces made of polyethylene terephthalate. Their structured surfaces consisted of nanocylinders of 160 nm height and 110 nm diameter [75]. However, different studies have shown different result regarding how topography influence the number of cells attaches on the surface. For instance, it has been shown in some studies that topography in micro scale increases the number of bacterial cells attached on the surface [6, 33]. While in the study has been done by M. Dineva, it has been observed that decrease in nanotopography results in increase in the number of bacterial cells attached on the surface [6]. Explanation for having more bacterial cells on the surface with topography can be the higher surface area available on nanostructured surface, protection from shear forces and chemical changes that cause preferential physicochemical interactions. Therefore, bacterial adhesion on surface features may increase the cell–surface contact area results in an increase in binding energy. However, the cost to bacterial cells in terms of elastic energy when adhering on the surface and the thermal energy in the environment may result in an energetic barrier to bacterial adhesion. This may be the reason why topography does not always result in more bacterial cells on the surface[6].

Therefore, it is possible that an optimal feature size for bacterial cells to adhere is at the microscale due to the limited capability of bacteria to deform. Moreover, when it comes to nanotopography one explanation can be that nano-roughness cannot be sense by bacterial cells and cannot affect the number of cells attach on the surface.

Furthermore, as it has been shown in fig. 18, the number of cells attached on both surfaces increased significantly at the early stage of experiment and it slowed down with time. The reason could be that at the early stage of the experiment the bacterial cells attached on the surface very firmly and there is no detachment of bacterial cells during the preparation of surface in order to be ready to analyze by SEM. While with time and when biofilm has formed many bacteria attach on biofilm loosely and there is a chance that they detach during the preparation process. However, further investigations are required to figure out the exact reason.

6.3. Fluorescence microscopy

The conclusion can be drawn from the results of the fluorescence microscopy (Fig. 22) is that nanotopography did not have any effect on the production of EPS. Different result has been observed in the study done by Mitik-Dineva et al [76]. In this study concanavalin A 488 dye (Molecular Probes Inc.) was used to label the extra-cellular polysaccharide (EPS) produced by three different bacteria including *P. issachenkonii, V. fischeri* and *P. aeruginosa*, on nanostructured glass surface modify via chemical etching. Confocal laser scanning microscopy was used to take images and the results have shown that there was more production of EPS on nanostructured surface[76]. The most interesting feature of the study done by Mitik-Dineva is that, they observed changes in the surface roughness might induce bacterial cells to produce different types of EPS during the attachment process[76]. Identification of the chemical composition of the EPS produced by *S.epidermidis* cells on both types of gold surfaces can be very helpful in order to find out if there is any difference between the type of EPS produced on flat and nanostructured surface.

As mention earlier, biofilm do not spread on the surface homogeneously and consequently stain penetration is not the same on the entire surface. Moreover, biofilm compose of several components with different chemical and biological properties that are still unknown [49]. Therefore, more sensitive analysis and further investigations are required to make a conclusion about the effect of nanotopography on the production of EPS. Moreover, since the dye has been used in study is a non-specific dye; it has stained any kind of protein including the one that exist on the cell membrane. Therefore, in the pictures taken from fluorescence microscopy it seems that cells are stain positive as well.

6.4. Quartz Crystal Microbalance with Dissipation Monitoring (QCM-D)

For further investigation on bacterial adhesion and EPS production QCM-D was applied. In Fig. 23 the first decrease in frequency for flat and nanostructured surfaces is due to adsorption of proteins present in bacterial solution from the beginning of the experiment as it also has been shown in fig 25.

Based on mass-loading theory and Sauerbrey equation, it is expected to see a negative frequency shift after the attachment of bacteria on the surface. However, a positive shift in third overtone for flat surface was observed. Similar result was observed in several other studied. For instance in the study has been done by A. Olsson et al. a positive frequency shift was observed for both S. epidermidis ATCC 35984 (EPS- producing) and S. epidermidis ATCC 12228 (non-EPS-producing) [70]. Because of positive frequency shift, one could assume that cells are detached from the surface. However result from SEM and fluorescence microscopy images show an increase of bacterial cells on both flat and nanostructured surfaces. The positive frequency shift can be explained by the coupled-oscillator theory instead of conventional mass-loading theory [70]. Based on equation 6 the resonance frequency of coupled-oscillator can be affected by spring constant (k) that relates to contact point stiffness. Less stiff contact leads to small k-values and consequently leads to positive frequency shift [70]. Therefore, this might indicate that bacterial cells did not attach to flat surface firmly in the beginning of the experiment that leads to small k-value and consequently positive frequency shift. No positive frequency shift for flat surface was observed in fifth and seventh overtones that can relate to difference in analytical depth between overtones. In fifth and seventh overtones, less area above the crystal was considered in order to measure the changes in frequency compared to third overtone and this

might results in negative frequency shift from the beginning of the experiment in fifth and seventh overtones.

The explanation for not having positive frequency shift on nanostructured surface at early stage of experiment can be because of firmly attachment of bacterial cells to the surface. Due to firmly attachment of bacterial cells to the surface the crystal and the bacterial cells will oscillate at the same frequency and lead to negative frequency shift.

The negative shift in frequency for flat surface after approximately 150 minutes indicates that the adhering mass and sensor surface are oscillating at the same frequency. This phenomenon can be because of bond maturation of bacterium-substratum with time that leads to firm attachment of bacteria on the surface. It has been shown by V.Rodriguezet al. through AFM studies that the force required to detach an adhered bacterium from the surface enhanced with time and the bacterium−substratum interface changes exponentially with time after the bacterial cells attach on the surface [77].

Another explanation for the negative frequency shift for flat surface after 150 minutes can be the formation of EPS that attach on the surface firmly (fig. 19) [70]. The attachment of EPS on the surface increases the adhering mass which based on equation 4, an increase on mass at constant value of k lead to a decrease in resonance frequency of the sensor-surface and is matched to the conventional mass-loading theory. Similar result was observed in the study done by A.olsson for the EPS-producing s.epidermidis strain that positive frequency shift changed to negative shift after almost one hour, indicating molecular adsorption according to conventional mass-loading theory [70].

The negative frequency shift for nanostructured surface can also be explained by mass-loading theory. An increase of adhering mass on the crystal and maturation of bacterium−substratum bond leads to negative shift in frequency.

As it was shown in result, changes in frequency were the same for flat and nanostructured surface after 150 minutes till the end of the experiment. Although no significant difference was observed between the final frequencies on both surfaces, it cannot be concluded that final mass on both surfaces is the same. The reason is that because the QCM-D measurements were done in the presence of water, an adsorbed biofilm may trap high amount of water that is count as a mass on the crystal [78]. It has been observed that the mass calculated by Saurbrey equation is higher than a real amount because it includes the water trapped in biofilm. The amount of water trapped in a biofilm can be as high as 95% and this amount depend on the type of surface and the type of molecule that are studied [78].

Changes in dissipation can give information whether the adhering mass is soft or rigid and this information cannot be achieved by looking only at changes in frequency. In this experiment, as shown in Fig. 24, dissipation was always higher on flat surface. Since the images provided by SEM showed that the number of cells attach on both surfaces was the same, this difference in dissipation likely relates to both how the bacterial cells interact with surface and the amount of EPS produced. It is possible that less bacterial cells survive on nanostructured surface, as they need to deform their structure in order to attach firmly and consequently less amount of EPS were produced. But as it has been shown in the research done by A. Olsson et al. the EPS production cannot influence the dissipation in large extent because they formed a rigid film on

the crystal [70]. Therefore, it is more likely that this difference in dissipation relates more to loosely attachment of bacterial cells on flat surface rather than more production of EPS.

Moreover, there is a constant increase in dissipation with time for both surfaces as expected since with time more bacteria will attach on the surface and more biofilm will be formed. This constant increase can also indicate the dissipation of the surface is affected by each bacterium that attaches on the surface [65]. The dissipation increases considerably at the early stage of the experiment, while with time it reaches the saturation level and is kept constant. A similar behavior was observed in the study done by A. Olsson for Three different *Streptococcus salivarius* strains [65]. This result can indicate rearrangements that occur in the interface between bacterial cells and the surface with time. Moreover, it is possible that water in the interface between the surface and bacterial cells has been removed because of an increase in the density of cell surface structures in the interface over time. With removal of water and interfacial rearrangements the number of contact points and interactions increase which lead to increase in adhesion strength between the bacterial cell and the substratum surface [65].

7. Conclusion

The main aim of this project was to study how nanotopography influences bacterial adhesion and EPS production. Images from Fluorescence microscopy showed that there is no difference in the amount of EPS produced on flat and nanostructured surfaces. However, it is possible that fluorescence microscopy is not sensitive enough to sense the difference. The QCM-D results have shown that dissipation is lower on nanostructured surface that can be due to firmly attachment of bacterial cells and more production of EPS. Therefore, bacteria seem to apply different strategies when adsorbing on a flat or nanostructured surface.

This study has shown that QCM-D has the potential to illustrate how bacterial cells interact with different surfaces. The result from QCM-D cannot be interpreted only through conventional mass-loading theory due to bacterial cell body and the coupled-oscillator theory must be applied in when interpreting the result [70].

8. Suggestions for further experiments

Some parts of the experiments can be improved. Below a summary of the most important suggestions for improvement are provided.

Recommendations for future surface preparations:

- Fabrication in clean room to avoid aggregation of particles on the surface due to contamination.

Recommendations for cell procedures:

- Use other type of bacteria with different appendage on their cell wall like pili or fellagela to see if they can influence the adhesion process. It is likely that since these appendages are in nanoscale, they can sense the nanotopography and influence the bacterial adhesion process.
- Compare non-EPS producing and EPS producing strain. By the use of non-EPS producing strain it will be easier to observe how bacterial cell interact with the surface.

Moreover, by this investigation, higher dissipation on flat surface can be better understood.

Recommendations for cell analysis:

- Perform one more type of staining on both surfaces in order to stain alive and dead cells on the surface. Applying this staining makes it possible to understand if cells can survive on nanostructured surface or not.
- AFM technique can be employed to measure the force of interaction between bacteria and surface. This technique is very useful to better understanding the interaction of bacterial cells with surface.
- Electrochemical impedence meaurements can be utilized in order to analyze the proteins and bacterial cells interactions with the surface using e.g. Layerlab Z1 instrument.

9. Acknowledgements

Project supervisors:

- **Hans Elwing-** provided the project and helped with some fundamental concept of the project
- **Mats Hulander-** helped with the overall plan and with most parts of the project
- **Mattias Berglin-** helped with the technique named dynamic light scattering and in some part helped to analyze the results

Additional assistance:

- **Anders lundgren** - helped with some part of the project
- **Emiliano pinori** - helped with imagej software and cell analysis
- **Ingrid johansson** - helped with cell culture

Examiner:

- **Julie Gold**- helped and supported during the project

10. References

1. Mariani, B.D. and R.S. Tuan, *Advances in the diagnosis of infection in prosthetic joint implants.* Molecular Medicine Today, 1998. **4**(5): p. 207-213.
2. Bengtson, S., *Prosthetic osteomyelitis with special reference to the knee - risk, treatment and costs.* Annals of Medicine, 1993. **25**(6): p. 523-529.
3. Chen, C.H.D., et al., *Controlled release of gentamicin from calcium phosphate/alginate bone cement.* Materials Science & Engineering C-Materials for Biological Applications, 2011. **31**(2): p. 334-341.
4. Etienne, O., et al., *Multilayer polyelectrolyte films functionalized by insertion of defensin: A new approach to protection of implants from bacterial colonization.* Antimicrobial Agents and Chemotherapy, 2004. **48**(10): p. 3662-3669.
5. Chen, W.C., et al., *Exploring antibacterial and antiadhesive activities of titanium surface modified with hydroxyapatite sol-gel containing silver*, in *Bioceramics, Vol 19, Pts 1 and 2*, X.D. Zhang, et al., Editors. 2007, Trans Tech Publications Ltd: Stafa-Zurich. p. 653-656.
6. Anselme, K., et al., *The interaction of cells and bacteria with surfaces structured at the nanometre scale.* Acta Biomaterialia, 2010. **6**(10): p. 3824-3846.
7. Natasa Mitik-Dineva, J.W., Radu C. Mocanasu, Paul R. Stoddart, Russell J. Crawford, Elena P. Ivanova Dr., *Impact of nano-topography on bacterial attachment.* biotechnology, 2008. **3**(4): p. 9.
8. McSwain, B.S., et al., *Composition and distribution of extracellular polymeric substances in aerobic flocs and granular sludge.* Applied and Environmental Microbiology, 2005. **71**(2): p. 1051-1057.
9. Dogsa, I., et al., *Structure of bacterial extracellular polymeric substances at different pH values as determined by SAXS.* Biophysical Journal, 2005. **89**(4): p. 2711-2720.
10. Díaza, C. (2006) *Influence of the Nano-micro Structure of the Surface on Bacterial Adhesion*. **10**, 4.
11. Mats Hulander, J.H., Marcus Andersson, Frida Gerven, Mattias Ohrlander, Pentti Tengvall, Hans Elwing, *Blood Interactions with Noble Metals: Coagulation and Immune Complement Activation.* applied material and interface, 2009. **1**(5): p. 10.
12. Leshem, R., et al., *The Effect of Nondialyzable Material (NDM) Cranberry Extract on Formation of Contact Lens Biofilm by Staphylococcus epidermidis.* Investigative Ophthalmology & Visual Science, 2011. **52**(7): p. 4929-4934.
13. Pavlova, A., et al., *Staphylococcus epidermidis and Pseudomonas aeruginosa adhesion intensity on a TiO(2) ceramic in an in vitro study*, in *Inter Academia 2010: Global Research and Education*, A. Medvids, Editor. 2011, Trans Tech Publications Ltd: Stafa-Zurich. p. 301-304.
14. Hu, Y.F., et al., *Adhesive properties of Staphylococcus epidermidis probed by atomic force microscopy.* Physical Chemistry Chemical Physics, 2011. **13**(21): p. 9995-10003.
15. Wang, C.Z., et al., *Role of spx in biofilm formation of Staphylococcus epidermidis.* Fems Immunology and Medical Microbiology, 2010. **59**(2): p. 152-160.
16. Nordqvist, C., *What Is Infection? What Causes Infections?* medical news today, 2010

17. Missirlis, M.K.a.Y.F., *Concise review of mechanismsof bacterial adhesion to biomaterials and of techniques used in estimating bacteria material interactions.* European cells and materials 2004. **8**: p. 21.
18. Nordqvist, C., *What Is Bacteria? What Are Bacteria?* Medical news today, 2009.
19. Heilmann, C., et al., *Molecular basis of intercellular adhesion in the biofilm-forming Staphylococcus epidermidis.* Molecular Microbiology, 1996. **20**(5): p. 1083-1091.
20. Todar, K., *Bacterial Structure in Relationship to Pathogenicity* in *Todar's Online Textbook of Bacteriology*. 2011: Madison. p. 2.
21. Beveridge, T.J., et al., *Functions of S-layers.* Fems Microbiology Reviews, 1997. **20**(1-2): p. 99-149.
22. An, Y.H.F., R. J., *Concise review of mechanisms of bacterial adhesion to biomaterial surfaces.* Journal of Biomedical Materials Research, 1998. **43**(3): p. 338-348.
23. Gristina, A. and H.H. Sherk, *Biomaterial-centered infection - Microbial adhesion versus tissue integration - (Reprinted from Science, vol. 237, pg. 1588-1595, 1987).* Clinical Orthopaedics and Related Research, 2004(427): p. 4-12.
24. E. B. H. Hume, a, b, c, d, J. Bavejaa, b, e, B. Muirf, T. L. Schuberta, b, N. Kumarg, h, S. Kjellebergh, i, H. J. Griesserf, j, H. Thissenf, R. Readg, h, L. A. Poole-Warrene, K. Schindhelme and M. D. P. Willcoxa, b, c, d, *The control of Staphylococcus epidermidis biofilm formation and in vivo infection rates by covalently bound furanones* Biomaterials, 2004. **25**(20): p. 8.
25. Hori, K. and S. Matsumoto, *Bacterial adhesion: From mechanism to control.* Biochemical Engineering Journal, 2010. **48**(3): p. 424-434.
26. Bader, D., Gilbert, Hasenwinkel, Henderson, Mather, Ren, Sureshkumar *control of bacterial biofilm formation*, in *http://lcs.syr.edu/academic/biochem_engineering/research_areas/biomaterials_tissue_engineering.aspx#a3*, BMCE Research Areas.
27. Cheng, G., et al., *Inhibition of bacterial adhesion and biofilm formation on zwitterionic surfaces.* Biomaterials, 2007. **28**(29): p. 4192-4199.
28. Weerkamp, H.J.B.a.A.H., *Specific and non-specific interactions in bacterial adhesion to solid substrata.* FEMS Microbiology Letters, 1987. **46**(2): p. 9.
29. Stenstrom, T.A., *Bacterial hydrophobicity, anoverall parameter for the measurment of adhesion potential to soil particles.* Applied and Environmental Microbiology, 1989. **55**(1): p. 142-147.
30. Vaudaux, P.E.F., P. Proctor, R. A. McDevitt, D. Foster, T. J. Albrecht, R. M. Lew, D. P. Wabers, H. Cooper, S. L., *use of adhesion-defective mutants of Staphylococcus-aureus to define the role of specific plasma- proteins in promoting bacterial adhesion to canine arteriovenous shunts.* Infection and Immunity, 1995. **63**(8): p. 3239-3239.
31. M., F., *The effects of proteins on bacterial attachment to polystyrene.* General Microbiology, 1976. **94**: p. 5.
32. Colon, G., B.C. Ward, and T.J. Webster, *Increased osteoblast and decreased Staphylococcus epidermidis functions on nanophase ZnO and TiO(2).* Journal of Biomedical Materials Research Part A, 2006. **78A**(3): p. 595-604.
33. Whitehead, K.A., J. Colligon, and J. Verran, *Retention of microbial cells in substratum surface features of micrometer and sub-micrometer dimensions.* Colloids and Surfaces B-Biointerfaces, 2005. **41**(2-3): p. 129-138.

34. Diaz, C., et al., *Nano/Microscale order affects the early stages of Biofilm formation on metal surfaces.* Langmuir, 2007. **23**(22): p. 11206-11210.
35. Mitik-Dineva, N., et al., *Differences in colonisation of five marine bacteria on two types of glass surfaces.* Biofouling, 2009. **25**(7): p. 621-631.
36. Scheuerman, T.R., A.K. Camper, and M.A. Hamilton, *Effects of substratum topography on bacterial adhesion.* Journal of Colloid and Interface Science, 1998. **208**(1): p. 23-33.
37. Elena Martines, K.S., Hywel Morgan, Nikolaj Gadegaard, Chris D W Wilkinson, Mathis O Riehle, *Air-trapping on biocompatible nanopatterns.* Journal Of Surfaces And Colloids 2006. **22**(26): p. 3.
38. Martines, E., et al., *Superhydrophobicity and superhydrophilicity of regular nanopatterns.* Nano Letters, 2005. **5**(10): p. 2097-2103.
39. Demann ET, S.P., Haubenreich JE, *Gold as an implant in medicine and dentistry.* pubmed, 2005. **15**(6): p. 12.
40. Weibo Cai, T.G., Hao Hong, Jiangtao Sun, *Applications of gold nanoparticles in cancer nanotechnology.* Nanotechnology, Science and Applications, 2008. **1**: p. 17.
41. Kimling, J., et al., *Turkevich method for gold nanoparticle synthesis revisited.* Journal of Physical Chemistry B, 2006. **110**(32): p. 15700-15707.
42. Biggs, S.M., P. Zukoski, C. F. Grieser, F., *Study of anion adsorption at the gold-aqueous solution interface by atomic-force microscopy.* Journal of the American Chemical Society, 1994. **116**(20): p. 9150-9157.
43. Chow, M.K.Z., C. F., *Gold sol formation mechanisms - role of colloidal stability.* Journal of Colloid and Interface Science, 1994. **165**(1): p. 97-109.
44. Chow MK, Z.C., *Gold Sol Formation Mechanisms - Role of Colloidal Stability.* Journal of Colloid and Interface Science, 1994. **165**: p. 13.
45. Jin, R.C., *Quantum sized, thiolate-protected gold nanoclusters.* Nanoscale, 2010. **2**(3): p. 343-362.
46. Martin, M.N., et al., *Charged Gold Nanoparticles in Non-Polar Solvents: 10-min Synthesis and 2D Self-Assembly.* Langmuir, 2010. **26**(10): p. 7410-7417.
47. Kooij, E.S., Brouwer, E.A. Martijn and Mewe, Agnes A. and Wormeester, Herbert Poelsema, Bene *Self-Assembly of Nanocolloidal Gold Films*. 2004, University of Twente Publications.
48. Grabar, K.C., et al., *Two-dimensional arrays of colloidal gold particles: A flexible approach to macroscopic metal surfaces.* Langmuir, 1996. **12**(10): p. 2353-2361.
49. Kumar, A., et al., *Linear superclusters of colloidal gold particles by electrostatic assembly on DNA templates.* Advanced Materials, 2001. **13**(5): p. 341-344.
50. S Gilles, C.K., M Pabst, U Simon, A Offenhäusser, D Mayer, *Patterned self-assembly of gold nanoparticles on chemical templates fabricated by soft UV nanoimprint lithography.* nanotechnology, 2011. **22**: p. 7.
51. *FilmTracer™ SYPRO® Ruby Biofilm Matrix Stain*, invitrogen, Editor.
52. *Staining bacterial biofilms: new uses for classic fluorescent dyes familiar probes take on a new role in biofilm staining.*, Invitrogen, Editor. 2007.
53. J., K. *The Material Science and Engineering* 2010.
54. Ian M. Watt, J.M., *The Principles and Practice of Electron Microscopy*. 1997.
55. Sartor, M., *Dynamic Light Scattering*, University of CaliforniaSan Diego: california.
56. *dynamic ligth scattering*, in *http://en.wikipedia.org/wiki/Dynamic_light_scattering*.
57. Caprette, D.R. *Principles of Spectrophotometry*. 2005.

58. Kirsten, M. *Spectrophotometry and Its Working Principle*.
59. *Essential parts of a spectrophotometer*, in *http://en.wikipedia.org/wiki/File:Spetrophotometer-en.svg*, Spetrophotometer-en.svg, Editor. 2008.
60. Richard M. Pashley, M.E.K., *Applied colloid and surface chemistry*. 2004.
61. *contact angle*, in *http://en.wikipedia.org/wiki/File:Contact_angle.svg*, Contact_angle.svg, Editor.
62. nikon, S.W.P., Thomas J. Fellers, Michael W. Davidson *confocal Microscopy, basic concept.* The source for microscopy education.
63. O'Sullivan, C.K. and G.G. Guilbault, *Commercial quartz crystal microbalances - theory and applications.* Biosensors & Bioelectronics, 1999. **14**(8-9): p. 663-670.
64. Fredrik Höök, B.K., *Variations in Coupled Water, Viscoelastic Properties, and Film Thickness of a Mefp-1 Protein Film during Adsorption and Cross-Linking: A Quartz Crystal Microbalance with Dissipation Monitoring, Ellipsometry, and Surface Plasmon Resonance Study.* American Chemical Society, 2001. **73**: p. 9.
65. Olsson, A.L.J., et al., *Novel Analysis of Bacterium-Substratum Bond Maturation Measured Using a Quartz Crystal Microbalance.* Langmuir, 2010. **26**(13): p. 11113-11117.
66. Edvardsson, M., et al., *QCM-D and Reflectometry Instrument: Applications to Supported Lipid Structures and Their Biomolecular Interactions.* Analytical Chemistry, 2009. **81**(1): p. 349-361.
67. Richard C. Ebersole, M.D.W. (1988) *Amplified mass immunosorbent assay with a quartz crystal microbalance*. 6.
68. Voinova, M.V., M. Jonson, and B. Kasemo, *'Missing mass' effect in biosensor's QCM applications.* Biosensors & Bioelectronics, 2002. **17**(10): p. 835-841.
69. Rodahl, M. and B. Kasemo, *On the measurement of thin liquid overlayers with the quartz-crystal microbalance.* Sensors and Actuators a-Physical, 1996. **54**(1-3): p. 448-456.
70. Olsson, A.L.J., et al., *Acoustic sensing of the bacterium-substratum interface using QCM-D and the influence of extracellular polymeric substances.* Journal of Colloid and Interface Science, 2011. **357**(1): p. 135-138.
71. Molino, P.J., et al., *The quartz crystal microbalance: a new tool for the investigation of the bioadhesion of diatoms to surfaces of differing surface energies.* Langmuir, 2008. **24**(13): p. 6730-6737.
72. Busscher, H.J., et al., *Interfacial re-arrangement in initial microbial adhesion to surfaces.* Current Opinion in Colloid & Interface Science, 2010. **15**(6): p. 510-517.
73. *QCM-D Technology*, qsense, Editor.
74. Wolfgang Haiss, N.T.K.T., Jenny Aveyard, David G. Fernig, *Determination of Size and Concentration of Gold Nanoparticles from UV−Vis Spectra.* ANALYTICAL CHEMISTRY, 2007. **79**(11): p. 6.
75. D Campoccia, L.M., H Agheli, D S Sutherland, V Pirini, M E Donati, C R Arciola, *Study of Staphylococcus aureus adhesion on a novel nanostructured surface by chemiluminometry.* The International journal of artificial organs, 2066. **29**(6): p. 9.
76. Mitik-Dineva, N.W., J.; Stoddart, P.R.; Crawford, R.J.; Ivanova, E.P, *impact of nano-topography on bacterial attachment.* Nanoscience and Nanotechnology, 2008. **3**(4): p. 9.

77. Virginia Vadillo-Rodrígueza, H.J.B., Willem Nordea, b, Joop de Vriesa, Henny C van der Mei, *Atomic force microscopic corroboration of bond aging for adhesion of Streptococcus thermophilus to solid substrata.* Journal of Colloid and Interface Science, 2004. **278**(1): p. 4.
78. Berglin, M., et al., *Use of surface-sensitive methods for the study of adsorption and cross-linking of marine bioadhesives.* Journal of Adhesion, 2005. **81**(7-8): p. 805-822.
79. Goetsch, V., Colloidal Silver An Analytical Investigative Report and Theoretical Overview. Free Online Colloidal Silver Ebook, Revised 2010. http://www.wishgranted.com/Colloidal_Silver_Pages_What_CS_is.htm

11. Appendix:

QCM-D measurements

These are the results from three QCM-D measurements on flat and nanostructured surfaces in three different overtones. All the conditions were exactly the same in all three measurements. The results show the changes in frequency and dissipation on crystal after the adhesion of bacterial cells with real time.

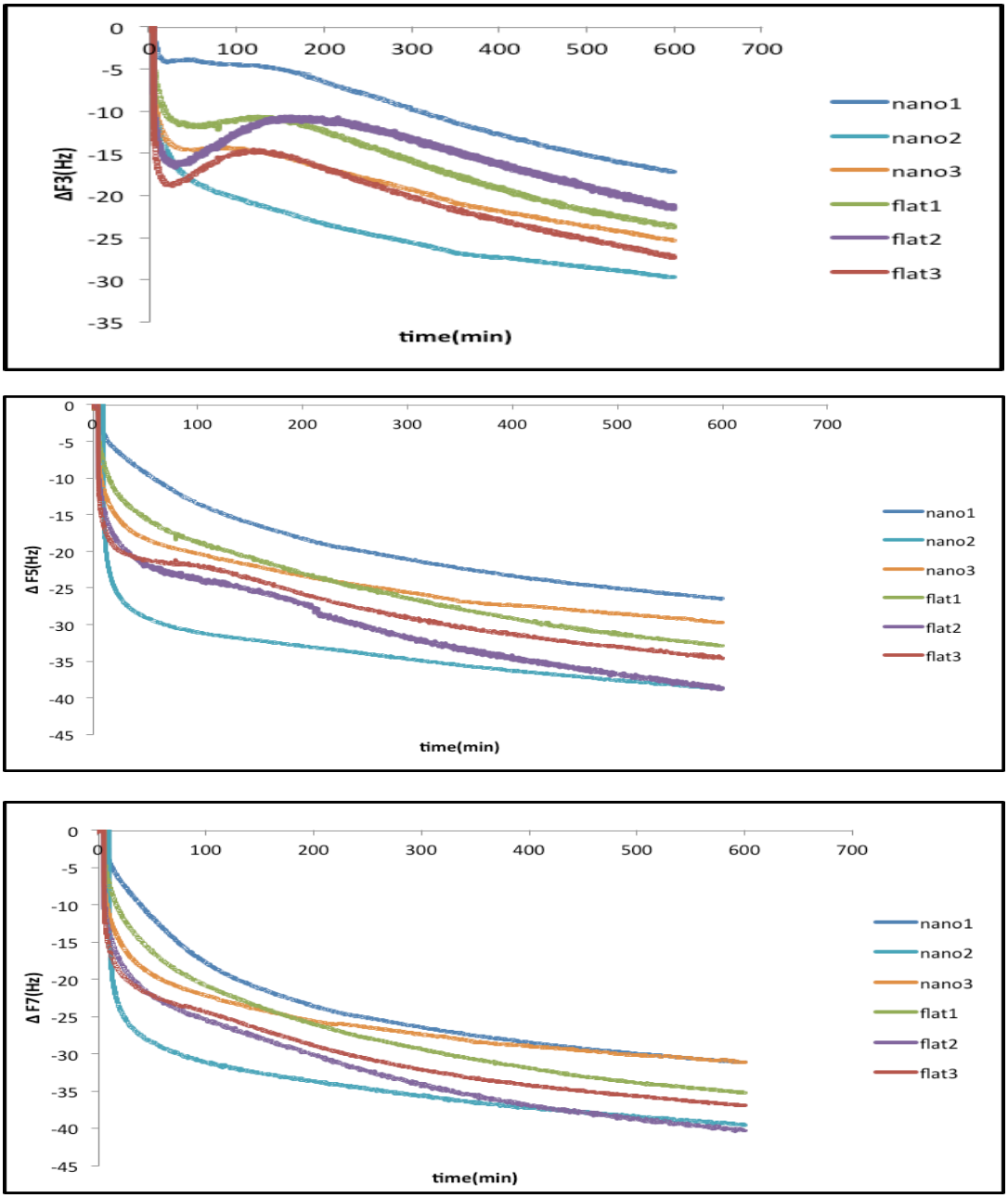

Figure 1. Changes in frequency on flat and nanostructured surfaces in three overtones for three different measurements.

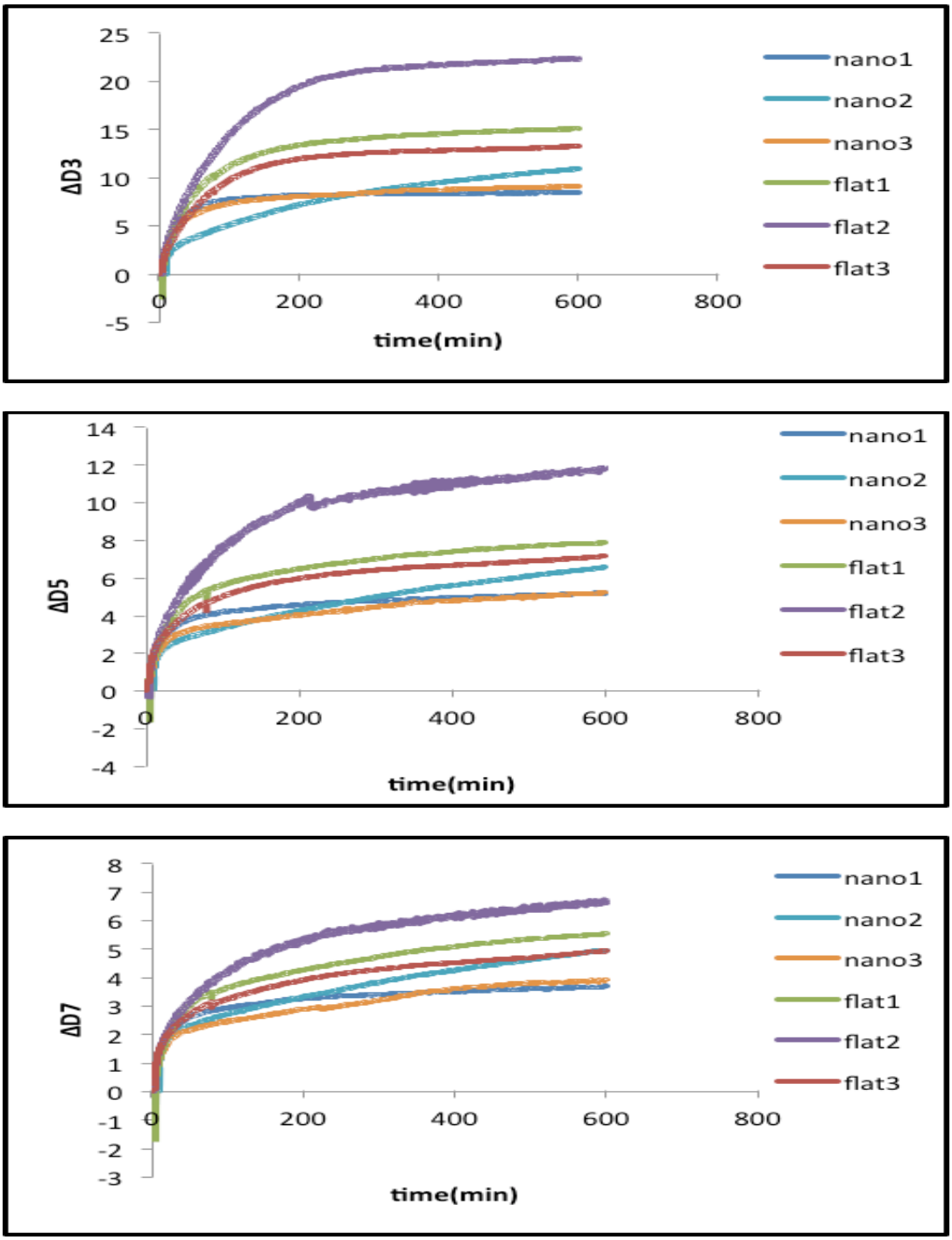

Figure 2. Changes in dissipation on flat and nanostructured surfaces in three overtones for three different measurements.

Imagej program

There were a group of steps were needed to be done on each image in order to get the data representing the amount of EPS on the surface. A program was design to perform all the steps on all the images. It was very essential to have the same exposure time and aperture for all images in order to be able to analyze the data.

The specific image is chosen

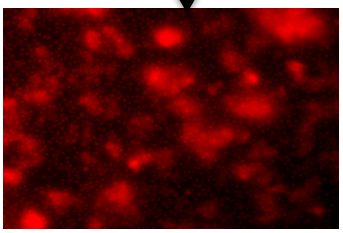

A histogram from image is provided

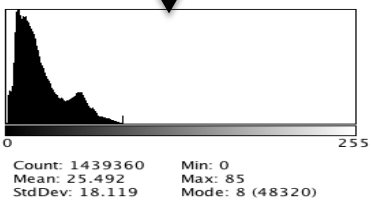

The program imageJ calculates the integrated intensity for all intensities. Integrated intensity is the multiplied of intensity and the number of pixels exist at that intensity.

Intensity	Pixel	Integrated intensity
0	613	Intensity × pixel
1	12186	
.	.	.
.	.	.
225	.	

Summation of all the integrated intensities is the output

Challenges with QCM-D technique

The condition that was consider stable in this project is not good because the QCM-D instrument used was very old and it was hard to achieve a completely stable condition. Moreover, since the equipment was old it was hard to control the temperature and in some experiments the result clearly shows that the temperature was not stable during the whole procedure (fig 3).

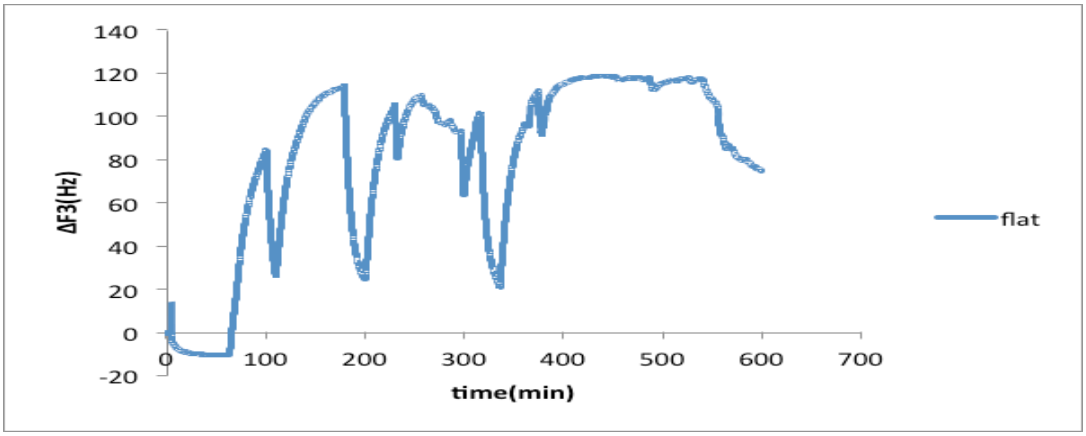

Figure 3. This graph shows an unsuitable QCM-D measurement because of changes in temperature.